Project acronym and title:
SECURe – Subsurface Evaluation of Carbon capture and storage and Unconventional risks

REPORT ON GEOCHEMICAL MODELS: LONG TERM EFFECTS OF CO2 AND METHANE LEAKAGE ON GROUNDWATER – DATA AND MODELS BASED ON TWO FIELD INJECTION EXPERIMENTS

Authors and affiliation:
Rasmus Jakobsen

Geological Survey of Denmark and Greenland, Øster Voldgade 10, 1350, Copenhagen K, Denmark

Email of lead author:
raj@geus.dk

Deliverable 2.4
Revision: 2 (corrected draft for definitive)

Disclaimer

This report is part of a project that has received funding by the *European Union's Horizon 2020 research and innovation programme* under grant agreement number 764531.

Project funded by the European Commission within the Horizon 2020 Programme	
Dissemination Level	
PU	*Public*
~~***CO***~~	~~*Confidential, only for members of the consortium (incl. the Commission Services)*~~
~~***CL***~~	~~*Classified, as referred to in Commission decision 2001/844/EC*~~

Deliverable number:	**2.4**
Deliverable name:	**Report on geochemical models: Long term effects of CO2 and methane leakage on groundwater – data and models based on two field injection experiments**
Work package:	**WP2 Risk assessment for leakage and induced seismicity: methodology and case studies**
Lead WP/deliverable beneficiary:	GEUS

Status of deliverable		
	By	**Date**
Submitted (Author(s))	**Rasmus Jakobsen**	**Nov. 16**
Verified (WP leader)	Elisa Calignano	Nov. 16
Approved (EB member)	Matteo Icardi	3/12/20
Approved (Coordinator)	Edward Hough	18.12.20

Author(s)		
Name	**Organisation**	**E-mail**
Rasmus Jakobsen	**GEUS**	**raj@geus.dk**

Public introduction

Subsurface Evaluation of CCS and Unconventional Risks (SECURe) is gathering unbiased, impartial scientific evidence for risk mitigation and monitoring for environmental protection to underpin subsurface geoenergy development. The main outputs of SECURe comprise recommendations for best practice for unconventional hydrocarbon production and geological CO2 storage. The project is funded from June 2018–May 2021.

The project is developing monitoring and mitigation strategies for the full geoenergy project lifecycle; by assessing plausible hazards and monitoring associated environmental risks. This is achieved through a program of experimental research and advanced technology development that includes demonstration at commercial and research facilities to formulate best practice. We will meet stakeholder needs; from the design of monitoring and mitigation strategies relevant to operators and regulators, to developing communication strategies to provide a greater level of understanding of the potential impacts.

The SECURe partnership comprises major research and commercial organisations from countries that host shale gas and CCS industries at different stages of operation (from permitted to closed). We are forming a durable international partnership with non-European groups; providing international access to study sites, creating links between projects and increasing our collective capability through exchange of scientific staff.

Executive report summary

Two experimental sites have been revisited to take samples for evaluating to what extent the aquifer chemistry had returned to its natural state following CO_2 injection/methane leakage. At the CO_2 injection site new samples showed that 7 years after the injection experiment the water chemistry 1.5 m downstream of the injection still had indications of ongoing cation exchange. This was confirmed by the composition of the cation exchanger which still showed signs of ongoing reequilibration of the cation exchanger. A 1D model set up in PHAST was fitted to the data up to 7 years, and used to assess the extent in time and space of a 1 year leakage event at a pressure of 5 atm in a system without carbonates and without silicate weathering. The model indicated that pH values down to a pH of 3 could be expected, but over time (100 yr) pH would largely return to preinjection conditions. The extent of the plume, though with small effects, was ~5-10 km. Any modelling of a specific site should use site specific data for both the geochemistry and the hydrogeology. At the CH_4 injection site the new samples showed that 4.5 years after the injection the water chemistry was very similar to the water chemistry before the injection, though there were still traces of methane and ethane from the injection. Sediment extractions also indicated that apart from Mn that appeared slightly depleted the sediment chemistry looked very similar to the situation before the injection. Due to the complexity of the distribution of both fluids and the gas phase after the injection a simplified batch model was used to calculate rates of methane oxidation, both the dissolved and gaseous methane, from pooled observations. The rate was then used to set up a simplified 1-D reactive transport model to assess the extent of spreading downstream. This was extended to a 100 day high rate leak resulting in a 300 m stretch of the aquifer with methane present in a gas phase. With the derived rates the model indicated that the methane could spread approximately 100 m downstream, but it should be noted that this requires the possibility of oxygen being supplied from above. In a methanogenic aquifer the spreading would not be limited by methane oxidation. For both the CO_2 and the CH_4 experiments, data show a low level of contamination of the groundwater and even if the contamination in relation to a larger leak should reach a water supply it appears that the contamination would be treatable using existing water treatment technologies used at water works.

Contents

FIGURES

TABLES

1 Introduction

One public concern with regards to CO_2 storage and unconventional production of CH_4 are the possible effects on the groundwater resources. To address this, experiments injecting CO_2 or CH_4 have been carried out during the last ~10 years . For this report a CO_2 injection site (Cahill *et al.*, 2014) and a CH_4 injection site (Cahill *et al.*, 2017) have been revisited to see if there are still effects of the controlled leakages in the groundwater and or the sediment. For the CO_2 site the injection took place ~7 years prior to the sampling, for the CH_4 site ~4.5 years had passed when it was resampled. Water samples and sediment samples were acquired and analysed and models describing the development on short and long term have been developed as described in the following.

2 Sites, prior experiments and new samples

2.1 CO_2 INJECTION SITE AT VRØGUM PLANTATION DENMARK

The CO_2 injection experiment took place in a shallow aquifer without any carbonate minerals, to see the extent of the effects of a leak, in what could be considered the most vulnerable in terms of producing acidification. The injection experiment and the following intense monitoring has been published in (Cahill *et al.*, 2014; Cahill and Jakobsen, 2015). The tested interval are the upper 10 meters of the sandy aquifer, where the top 4 m are aeolian sand, overlying meltwater sand.

2.1.1 The Vrøgum Plantation CO_2 injection experiment

In the experiment 1600 kg of CO_2 gas was injected during a period of 72 days at 4 and 10 mbs (meters below surface) into the lower marine sand and monitored in a network of downstream samplers. Water samples were taken 3 times prior to the injection and 10-12 times during and after the injection, depending on the specific sampler and the migration of the plume.

2.1.2 New samples from Vrøgum and analytical methods

Water samples and sediment samples for this study were taken from two positions 1.5 m downstream of the injection from 2-8 mbs through the zone where the largest effects of the CO_2 were seen during the first monitoring period following the injection. Water was analysed for pH and EC (electrical conductivity) using electrodes in the field. Major anions were measured by Ion Chromatography and cations as well as trace elements were measured by ICP-MS. The ICP-MS measurements were done using the same preparation and methods as in Cahill *et al.* (2014). Alkalinity was determined by titration in the lab of the sample in the vial that the sample was filtered into to include possible precipitates in the titration. Sediment samples were extracted targeting surface bound ions as well as Fe-oxides and trace elements associated with these. The extraction solutions also dissolve other parts of the sediment to varying degrees, but since the purpose here is to examine changes related to the CO_2 injection, in samples that are very similar in composition, this is acceptable. In fact, it is not important exactly what minerals are extracted. The extraction solutions used were $NaHCO_3$ (pH 8.5) which releases loosely surface bound ions, Formic acid (pH 3) which dissolves very unstable Fe-oxides and releases ions that may exchange with H^+, NH_4-oxalate (pH 3) – dissolving unstable oxides, ascorbic acid (pH 3) – dissolving slightly stable oxides, and NH_4-oxalate + ascorbic acid (pH 3) which extract stable oxides such as goethite. The extraction solutions were the same as those used by Cahill *et al.* (2014) enabling a comparison. Exchangeable cations were determined using 1M NaCl and NH_4Cl solutions as described in Cahill *et al.* (2014). The NH_4Cl solution is used to determine all exchangeable ions except NH_4^+, this makes it possible to measure the extracts by ICPMS. Exchangeable NH_4^+ is determined from the NaCl solutions.

2.2 CH_4 INJECTION SITE AT BORDEN, ONTARIO CANADA

The methane injection experiment used a carbonate-bearing Pleistocene beach sand aquifer. Details and results from the experiment until 245 days and 700 days after start of the injection are given in Cahill *et al.* (2017) and Forde *et al.*, (2019) respectively.

2.2.1 The Borden CH_4 injection experiment

In the Borden CH_4 experiment, 36.4 kg of CH_4 (51 m^3 at STP) was injected over 72 days at 0.17 (28 days), 1.0 (40 days) and 4.3 m^3/h (2 days) at 4 and 8 mbs and the plume was monitored in a network of downstream samplers. Water samples were taken 1-3 times (depending on the sampler) before injection started and up to 20 times after the injection started, depending on the position in the network relative to where the effects of the migrating methane were seen.

2.2.2 New samples from the Borden site and analytical methods

Water samples and sediment samples for this study were taken in the samplers in the starboard (right looking in the direction of flow) side of the experimental field where previous sampling showed the latest and highest CH_4 concentrations and the most significant effects on other parameters. Most of the new samples taken were taken 2 mbs where the data from 700 days after the injection showed the most pronounced effects on the water chemistry. Samples were analyzed using the same methods and lab as used before (Forde *et al.*, 2019). Briefly, water samples were analysed for temperature, pH, dissolved O_2, ORP and EC in the field using electrodes. Alkalinity was measured in the field by titration. Gas samples were measured by GC. Cations and trace elements were measured by ICP-MS and ^{13}C of CO_2 and CH_4 were measured by IRMS. Sediment extractions were done using a subset of the same extraction solutions used for the Vrøgum field site (Formic acid (pH 3), NH_4-oxalate (pH 3), ascorbic acid (pH 3) and NH_4-oxalate + ascorbic acid (pH 3), however in the extractions done on the Borden samples prior to and after injection the high carbonate content was not taken into account, limiting the extraction efficiency and the possibilities of comparing before and after. A comparison on new core material taken for this study, between an extraction using formic acid, as it had been done previously, where the amount of formic acid was too low, with the results from an extraction of the new core material, using an adequate amount of formic acid, indicated that the element concentrations in the two extracts were highly correlated and when the element concentrations were divided by the Fe content the distribution was very similar. This was not the case for the other extractants and therefore, a before and after comparison has only been made on the results of the formic acid extractions.

3 Results

3.1 RESULTS FROM THE CO_2 INJECTION EXPERIMENT SITE (VRØGUM)

The main effect observed during the injection experiment was a lowering of the pH due to the formation of carbonic acid. This triggered dissolution of $Al(OH)_3$, presumably gibbsite, which triggered cation exchange reactions where the Al exchanged for the cations on the exchanger, primarily Ca, Mg and K but also Na to a minor extent. In the following the results from the new sampling at the Vrøgum site, are compared with the results from the monitoring data from the injection experiment focussing on parameters that indicate to what extent the system still shows signs of the injection experiment.

3.1.1 Water chemistry

Comparing the water chemistry 7 years after the injection with the average water chemistry of the background samples taken before the injection started indicates that the differences are generally rather small and values are both lower and higher than the initial background for most of the sample positions. A few positions exemplified by the M8 sampler water chemistry shown in Fig. 1 show systematic deviations in the cations and pH – presumably due to a higher CEC (Cation Exchange Capacity) implying the exchanger has still not equilibrated with the background water.

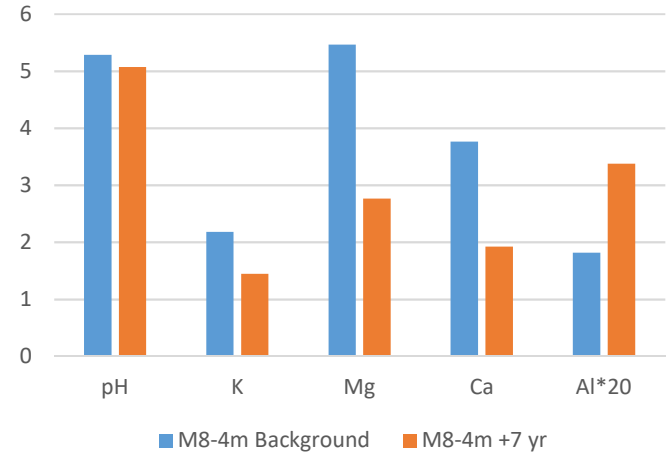

Figure 1: Average background values (blue) of pH and cations (mg/L) from sampler 1.5 m downstream of injection compared with measurements made 7 years after the injection (orange).

The Al concentration is slightly higher in the +7 years samples, indicating that Al is still being released from the exchanger, while the concentration of the other cations are lower in the +7 years samples, indicating that they are still being bound to the exchanger. The Al released from the exchanger will tend to precipitate as Gibbsite ($Al(OH)_3$) thereby lowering the pH, which fits with the slightly lower pH in the +7 years samples. Major anions such as Cl^- , and SO_4^{2-} show differences between before and after the injection, but these are not systematic, presumably these are influenced by variations in the input of sea spray because the site is situated just 6 km from the west coast of Denmark.

3.1.2 Sediment Chemistry

The exchangeable cations (Fig. 2) show a pattern that corresponds to the pattern observed in the water chemistry from the sample position shown in Fig. 1. The exchanger still has a higher equivalent fraction of Al compared to the background while the equivalent fractions of the other ions (except for Mg in the outwash sand) is lower than before the injection.

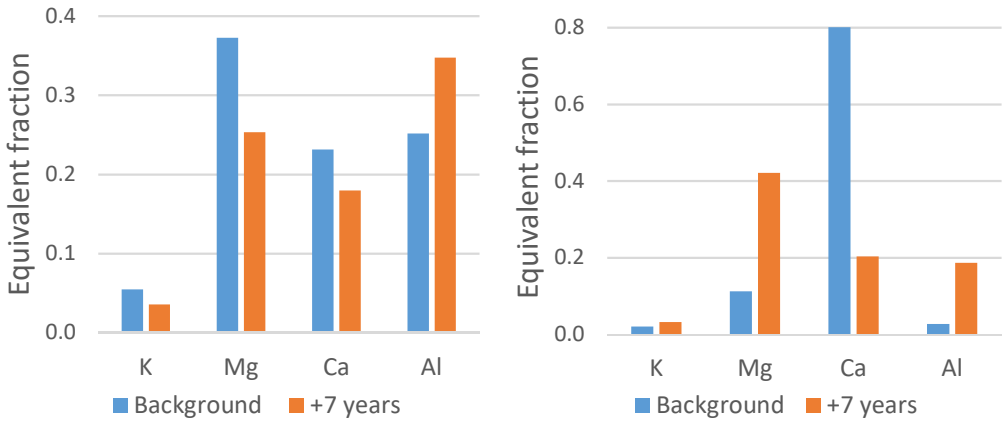

Figure 2 The distribution of exchangeable cations before (blue) and 7 years after (orange) on the eolian sand (left) and outwash sand (right), 1.5 m downstream of the CO_2 injection.

The fact that the effects of the 72 day CO_2 injection is still visible in the water and sediment chemistry 7 years after may seem surprising, but is a consequence of the very dilute water at the site and an ion exchanger capacity which, compared to e.g. a soil is very low, but recalculated into mmol exchanger sites per liter of groundwater is around ~75 mmol/L, while the total amount of cations in the water is only around 1.5 mmol/L.

An extraction procedure targeting loosely bound elements released by $NaHCO_3$ and Fe-oxides of increasing stability (see methods section) and the trace metals bound to these was carried out before, 143 days, and 7

years after the injection start. In order to remove the variation in the data related to variations in mineralogy and the Fe-oxide content the 2-3 samples from the aeolian and the outwash sand were averaged and all the other ions included in the analysis have been divided by the amount of extracted Fe, except for the $NaHCO_3$ extracts where Ca was used for normalisation since this step does not dissolve any Fe-phases, but is more similar to an exchange (Fig. 3). The changes seen are relatively small, for the aeolian sand they are probably too small to warrant any interpretation. For the outwash sand the extracts in formic acid, ascorbic acid and oxalate+ascorbic acid there appears to be a clear increase from before the injection to 143 days after the injection followed by a decrease to the samples taken 7 years after the injection. For most elements it appears that the values are slightly higher than they were before the injection. In contrast to the major cations this difference is not visible in the water chemistry. Considering that the effects as they appear in the data from the oxalate extractions look quite different, with most parameters higher in the extracts from before the injection indicate that one of the effects of the injection and presumably the acidification has been a recrystallization of the Fe-oxide phases. Without more detailed investigations it is, however, difficult to determine whether this is the case. The results indicate that the subtle changes in the sediment chemistry caused by the injection are still visible 7 years after the injection.

Figure 3: Results from the extraction of aeolian and outwash sediments. The values have been divided by the amount of extractable Fe, except for the $NaHCO_3$ extracts where Ca was used for normalisation

3.2 RESULTS FROM THE CH_4 INJECTION EXPERIMENT (BORDEN)

The injection of methane took place at two different depths (4 and 8 mbs). Due to the low solubility of CH_4 it dispersed as a gas phase far faster than the water in the system. The complexity of this is described in (Cahill *et al.*, 2017). As described above the injection of CH_4 took place at three different rates. At all stages it was clear that due to the migration of the CH_4 as bubbles the spreading within the aquifer was somewhat erratic, especially after the last most rapid phase of the injection. In the following the focus is on the situation 2 mbs as this is where most of the samples from the sampling undertaken for this study were taken (day 1597), because this is where there were the clearest indications of effects from the injection in the samples taken on day 700. As for the Vrøgum site the focus is on data that can indicate to what extent the system has returned to background conditions.

3.2.1 Water chemistry

Though the focus is on the extent to which effects of the methane can still be seen, the complexity of how the CH_4 spread within the aquifer has implications for the interpretation used for the modelling. To illustrate the complexity, the entire series of methane measurements from screens 2 mbs are shown in Fig. 4. The methane was injected at 4 and 8 mbs implying that there is some delay between the changes in injection rate and the response and since the methane migrates as a gas phase, concentration variations are erratic. It appears that for the first 28 days where the injection rate was 0.173 m^3/day (split evenly between 4 and 8 mbs) the concentration stabilizes somewhat indicating that already at this point there is some methane oxidation going on. After 28 days the injection rate was increased to 1 m^3/d (0.5 m^3/d at each depth) which led to a short period of very high concentrations which appear to drop off, perhaps again due to methane oxidation. On day 70 the injection rate was set to 4.3 m^3/day which leads to intrusion of CH_4 over a larger area with concentrations and extent peaking at day 113. Following this it appears that a high concentration in the water is maintained for an extended period, indicating that a gas phase trapped in the sand as bubbles is dissolving into the water over time. The contours, though with considerable uncertainty due to lack of data points at X>2 m, indicate that a large part of the methane is found outside the monitoring system. Both the shape of the contours, resembling what was seen at day 700, as well as the concentrations indicate that there are still faint traces of the injection on day 1597. The data from day 496 indicates that a new portion of CH_4 has migrated into the monitoring field from the starboard side and it appears to be remnants of this that are visible at day 700 and 1597. The $\delta^{13}C$ values in the methane seen at day 496 and 700 indicate that it is the injected methane. The concentrations seen at day 1597 are only slightly above the background concentrations from day -49, indicating that we are very close to being at the end of the period in which the effects of the CH_4 injections can be seen in the water chemistry.

The $\delta^{13}C$ of the low amounts of methane gas found in the samples from day 1597 did not correspond to the $\delta^{13}C$ of the injected gas, but had values in between the value of the injected gas and the background biogenic methane, one sample had a value very close to the biogenic methane. It could indicate that the intrusion of methane had produced fresh organic matter in the form of methane oxidizing biomass, and when the methane is gone this reactive organic matter may be used in producing biogenic methane, thereby prolonging the presence of methane at very low concentrations.

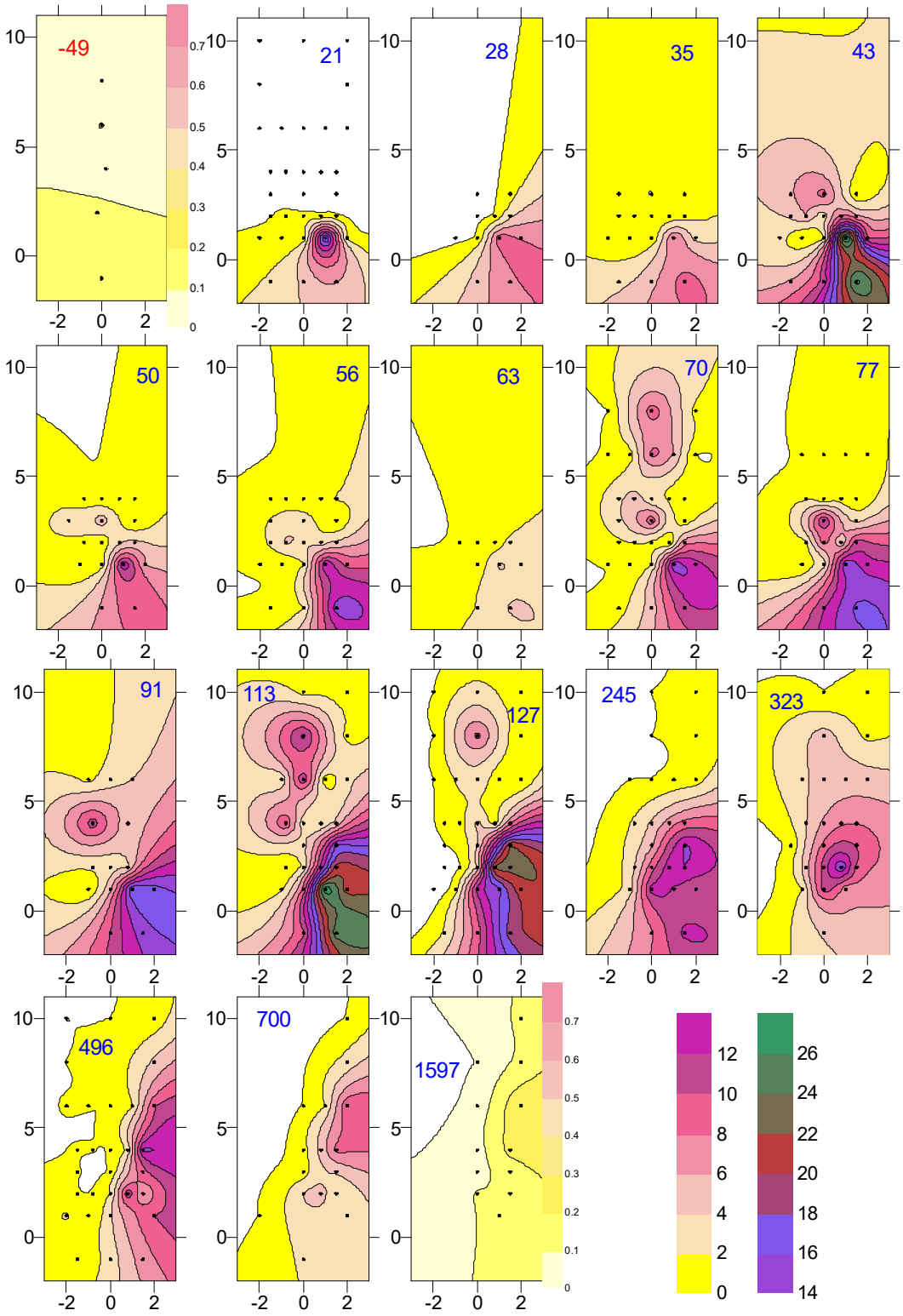

Figure 4: The methane concentration (in mg/L) before during and after the injection at 2 mbs. The injection took place at 4 and 8 mbs. Day number in blue, note that days -49 and 1597 have concentration scales that are different from the rest, shown in the lower right corner.

In terms of reactions caused by the methane the erratic distribution makes it difficult to clearly see these in plan view. The clearest impression is seen on 1D longitudinal plots through the monitoring field as shown in Figure 5 for Ca 2 mbs from samplers in a transect in the direction of flow.

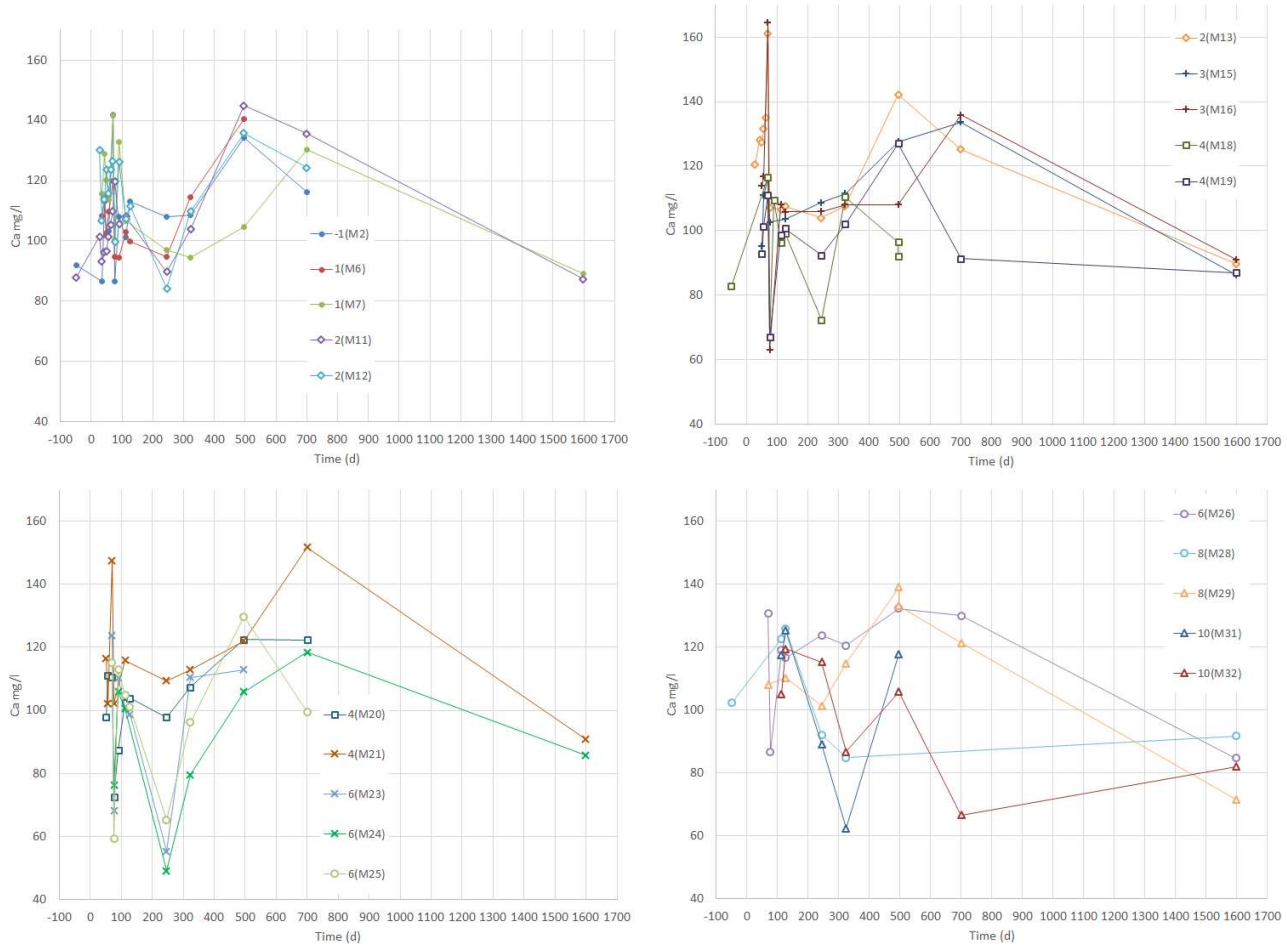

Figure 5: The development in the Ca concentration in the general flow direction of the test field from samplers 2 mbs. The first number in the legends is the distance in m in the direction of flow from the injection.

From day 245 until day 700 there is a clear increase in Ca in most of the samplers within 8 m from the injection indicating dissolution of calcite. The dissolution of calcite is presumably caused by the CO_2 produced by methanogenesis as illustrated in Eq. 1.

$$CH_4 + 2O_2 + CaCO_3 \Rightarrow Ca^{2+} + 2HCO_3^- + H_2O \quad (1)$$

In this context it is worth noting that at day 1597 where the samples for this study were taken the Ca concentration is close to the background values observed prior to methane injection. A similar pattern is seen for Mg, presumably because the $CaCO_3$ dissolving is not a pure calcite but contains Mg substituting for Ca in the Mg-calcite.

The dissolution of carbonate buffers the pH, implying that only small changes are seen (Fig.6). Erratic changes are seen in the beginning, also seen for Ca, which has been interpreted (Cahill et al., 2017) as an effect of water being drawn up and mixed in from below by the CH_4 bubbles coming from the injections below. Here it seems that the pH at 1597 days after the injection start is actually slightly lower than the initial values at day -49, before the injection. The change appears to be around 0.4 pH units. The alkalinity of the system also varies (not shown), but the general level is not systematically different at day 1597 compared to day -49. Since the pH in natural circumneutral systems is normally a function of the ratio between carbonic acid and bicarbonate, and bicarbonate is close to equivalent to the alkalinity, it implies that the level of carbonic acid is slightly higher at day 1597, meaning that the total amount of inorganic carbon dissolved in the water is higher than before the injection.

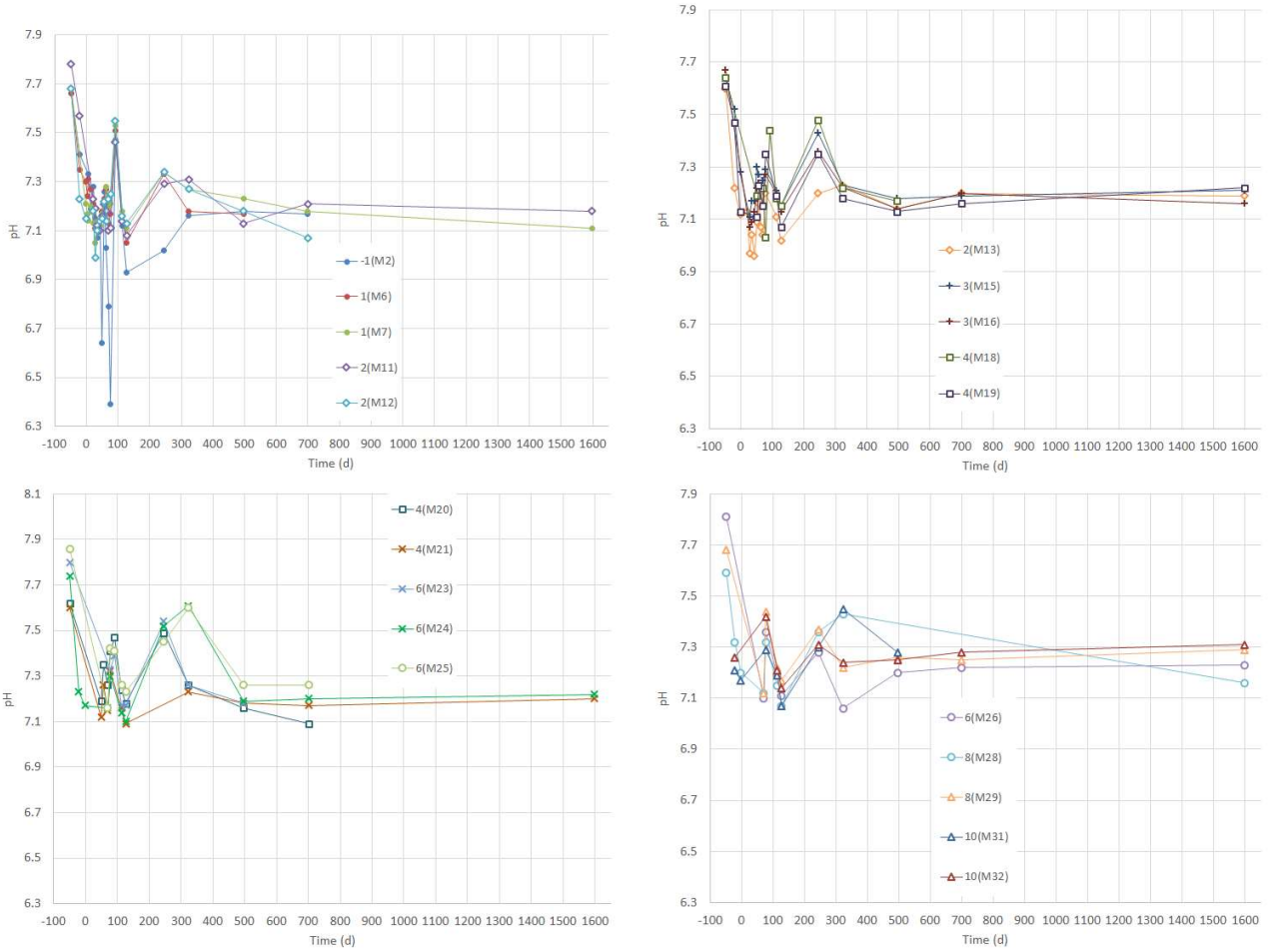

Figure 6: The development in the measurted pH in a transect the general flow direction of the test field from samplers 2 mbs. The first number in the legends is the distance in m in the direction of flow from the injection.

Notable in a groundwater quality context is an increase in several trace elements in what appears to be a very sharp peak, though this is mostly due to the long spacing in time between sampling. The increase is most clear for Ni shown in Fig. 6. Similar patterns are seen for As and Zn, and to some extent Al, though not as clear.

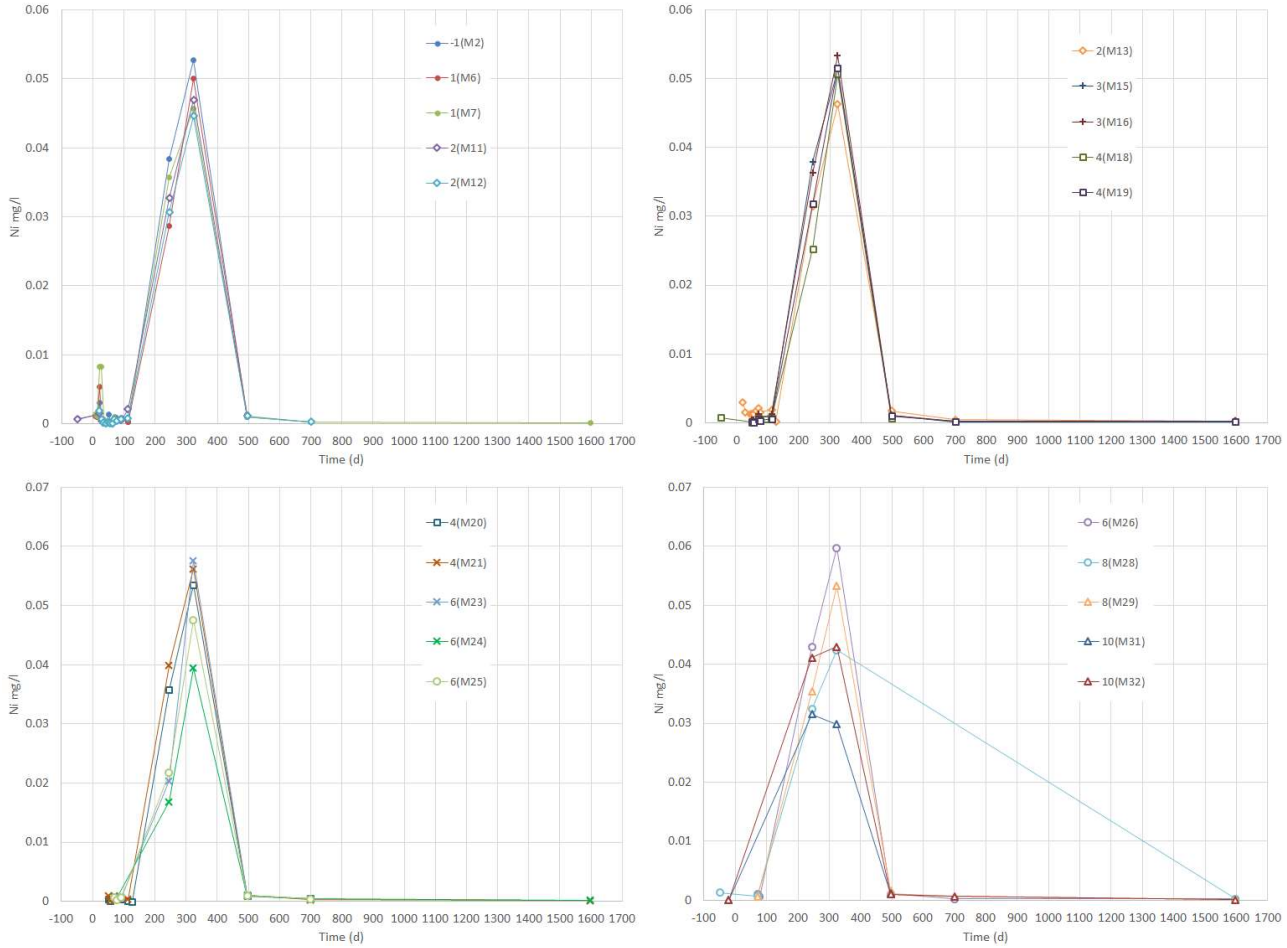

Figure 7: Ni concentration over time in a transect 2 mbs in the direction of flow. The first number in the legend is the distance in m relative to the injection position.

From day 127 to day 323 the Ni concentration increases from the very low background concentration to around 50 µg/L for some of the samplers. This is above the drinking water limit, but presumably standard aeration causing precipitation of Fe- and Mn-oxides would also take out the trace elements by adsorption to the formed oxides. The source of the elevated trace elements could be reductive dissolution of Mn-oxides which can contain large amounts of trace elements, however, though there is an increase in the Mn concentration it comes later, but crossplots of Ca and Mn do not indicate that the increase in Mn is related to the increase in Ca from carbonate dissolution. The lack of synchronization between the trace metal peak and the increase in Mn could be due to an interference from precipitation of rhodochrosite ($MnCO_3$), but based on the available data, this conclusion is tentative. Again in terms of how long effects of leaking CH_4 would be visible in the groundwater, the trace metal peak is short and there are no traces of it at day 700, nor at 1597 days.

3.2.2 Sediment Chemistry

The useful data for the sediment chemistry are limited, as described in the methods section, but as described, it appears that the extracts made with formic acid are comparable when normalized by the amount of extracted Fe as it was done for the Vrøgum samples (Fig. 8). Generally, the changes from before injection, post injection and 4.5 yrs after the injection are small. it seems that for a lot of the elements the element/Fe ratio 245 days after the injection is lower, for example the Ni/Fe ratio is low at day 245, which is also when the first high concentration in the porewater is measured. It also appears that the Mn/Fe ratio decreases over time which could support that the higher trace element concentrations are related to Mn-oxide reduction. In terms of the context of the amount of time it would take for the entire system to return to background conditions, there are several element/Fe ratios that are quite close to background values at day 1597, but for some elements the ratio is still low after 1597 days, most obvious for Mn/Fe. If Mn-oxides have been dissolved and some of the Mn has been transported away from the site as dissolved Mn, conditions exactly like they were prior to the

injection can probably not be reached. This is not necessarily a problem, because the net effect on the groundwater chemistry will be quite small.

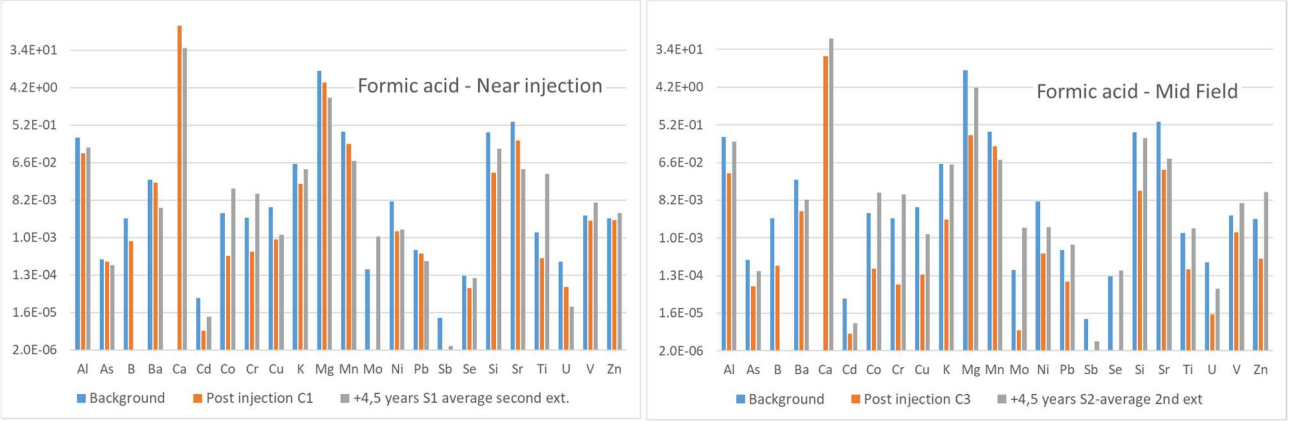

Figure 8: Results of extracting sediment from 2 mbs in formic acid (pH 3). Values are normalised by dividing the concentration of the given element with the concentration of Fe.

4 Modelling

4.1 PHREEQC/PHAST MODEL FOR THE CO_2 INJECTION SITE (VRØGUM)

The Vrøgum site was modelled previously using a 1-D PHREEQC (Parkhurst and Appelo, 2013) reactive transport model (Cahill and Jakobsen, 2015) and this model was used as a starting point for the model used here. The main aim of the modelling work has been to give a way of extrapolating the injection experiment in time and space for the actual injection experiment, but also for a longer CO_2 release and a different depth of release.

4.1.1 CO_2 injection experiment model setup

Where the model from Cahill and Jakobsen (2015) used an equilibrium model with two different gibbsite reactivities, the new model uses a kinetic description of the gibbsite dissolution using the compilation of kinetic expressions for PHREEQC in Zhang *et al.* (2019) implementing equations and parameters from Palandri and Kharaka (2004). The equation includes a surface area parameter, and in order to fit the data this had to be increased to 4800 m^2/g which appears to be unrealistically high indicating that the rate constant in the data from Palandri and Kharaka is too low. Also, the exponent to the ratio of mass left to the initial mass was increased to 2.5, implying that the rate decreases more as more has reacted. Another difference compared to the Cahill and Jakobsen paper is the inclusion of a Ba-bearing amphibole in an attempt to model the increase in Ba seen in the data. We do not know that the source of Ba is amphibole, it could be many other minerals e.g. muscovite. As the model results shown in the following show, the effect that could be obtained using a realistic Ba content of 5% was small. The Cahill and Jakobsen (2015) model includes surface complexation using the CD-MUSIC model (Hiemstra and Van Riemsdijk, 2006) implemented in PHREEQC using the database compiled by Jessen *et al.* (2012). In addition, the model includes cation exchange using the exchange parameter derived by Cahill and Jakobsen based on measurements of groundwater composition and determination of exchangeable cations of associated sediment. The time for calculating the models was long using PHREEQC, so in order to speed up the calculation the 1D PHREEQC model was implemented as a 1D PHAST model which can use multiple processors using a scheme where the geochemical calculations are done in parallel and once the geochemical calculations are finished the water is moved in a transport step.

4.1.2 Model results for the injection experimental period

All inorganic elements measured in the groundwater are included in the modelling. The fit is made manually, and the goodness of fit is evaluated visually. It turns out to be impossible to make a good fit of all parameters, so emphasis is put on obtaining a good match for Al, pH and alkalinity. The fit obtained for these parameters over time at 1.5 m downstream are plotted in Fig. 9, together with a number of other parameters; cations controlled by the cation exchange, and Si largely controlled by the surface complexation. Ba turns out to be

difficult to fit, unless the Ba-bearing amphibole or another silicate phase with Ba is made very Ba-rich, otherwise the Si cannot be fitted.

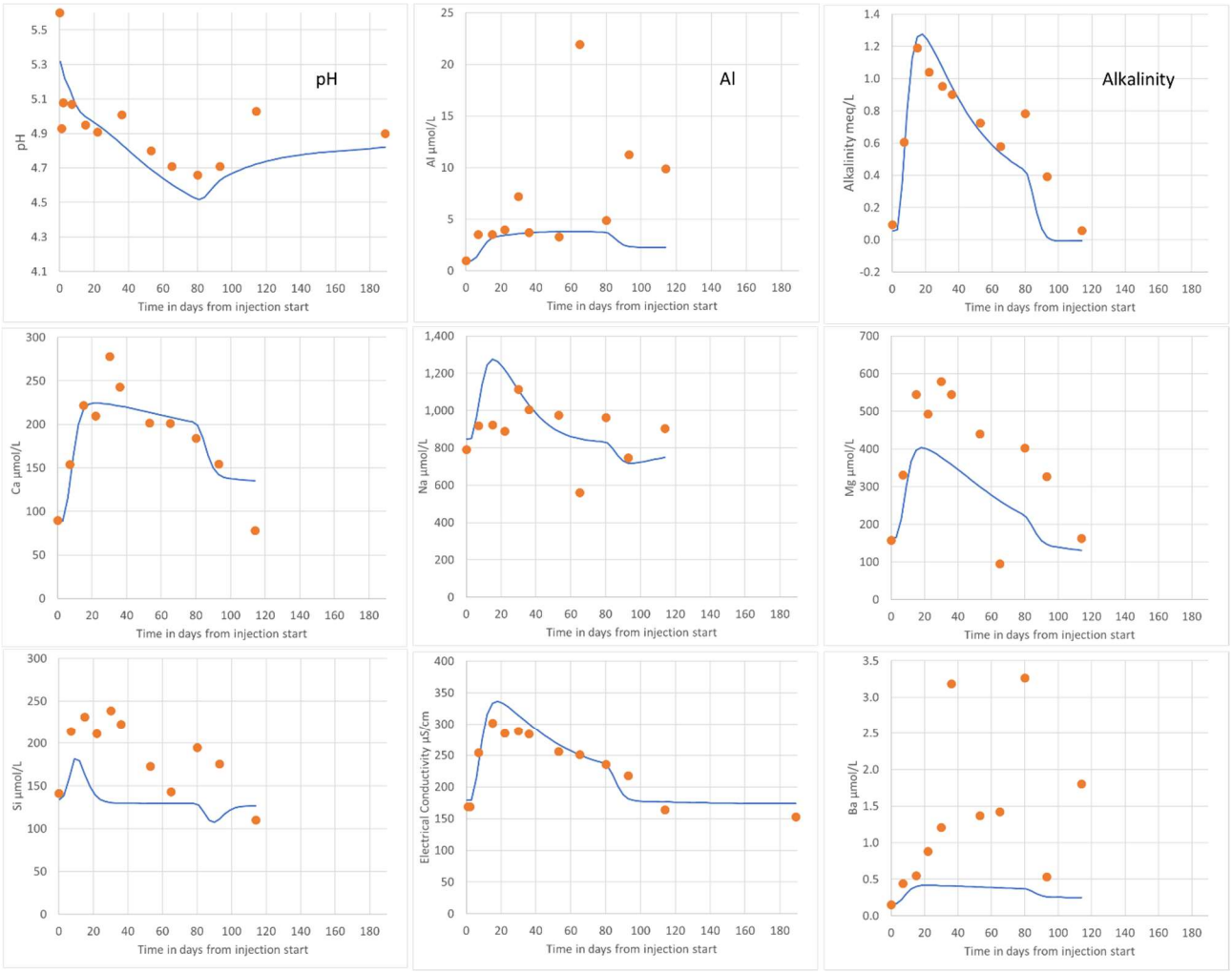

Figure 9: Model (blue line) and observations (orange dots) from 1,5 m downstream of the injection at 6 mbs for 9 parameters

Al, pH and alkalinity are plotted as a function of distance relative to the injection and at different times in Fig. 10 using the same parameters used for the fit in Fig. 9. It turns out that the fit over distance is not as good and could not readily be improved using the same set of parameters. For example, the high measured values for Al are difficult to match, which most probably relates to a variation in the reactivity in the gibbsite and since the gibbsite dissolution is the most important process, this affects all other parameters. In addition, there are probably also variations in the cation exchange capacity as well as selectivity coefficients which will also affect the behaviour of Al and presumably explains why the cation concentrations also show a poor fit to the measured data when viewed in the spatial dimension (not shown).

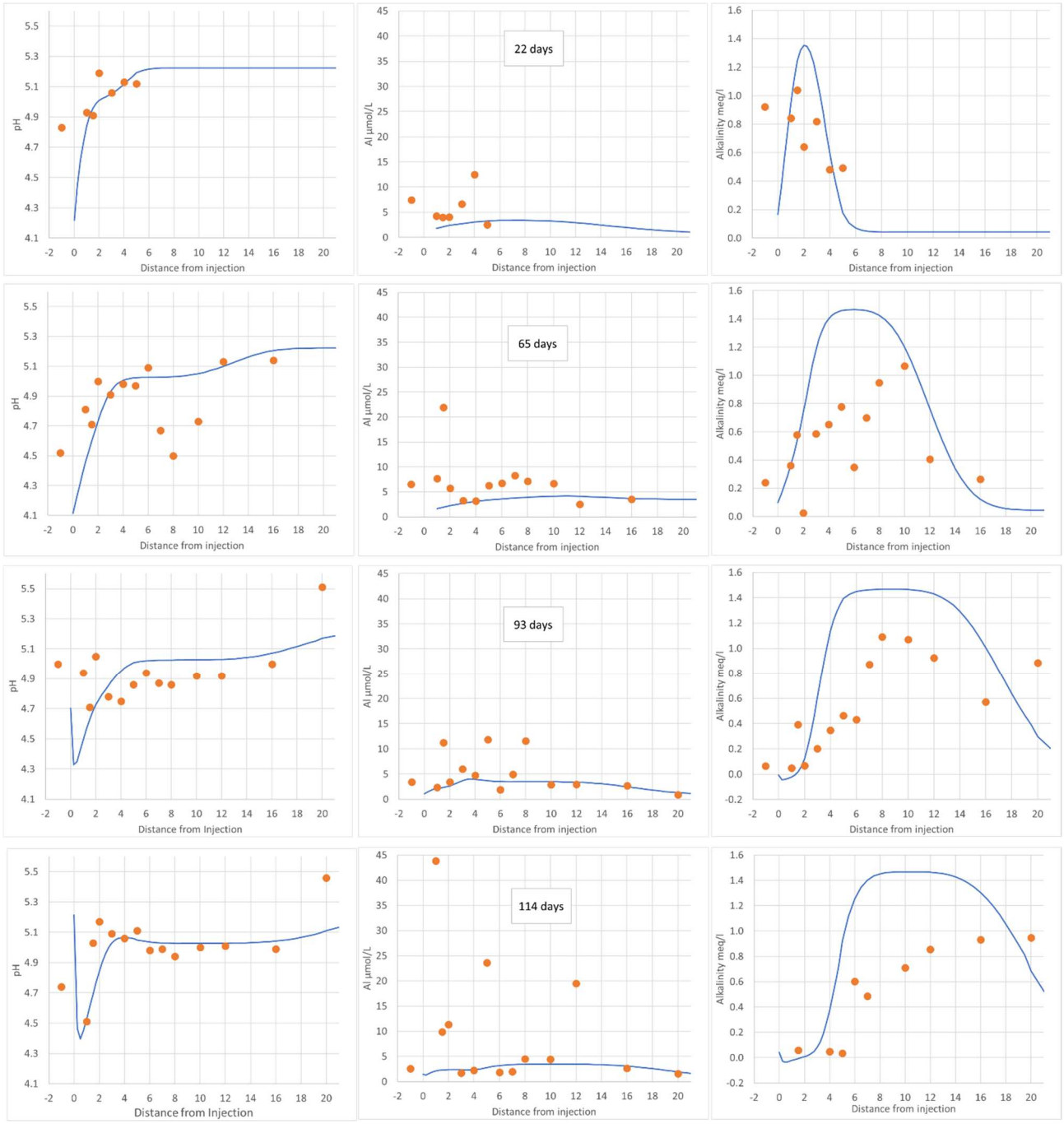

Figure 10: The pH, Al and alkalinity from a 1-D transect at 6 mbs, through the plume created by the CO_2 injection at different times.

4.1.3 Extrapolations of the model

The model matched to the detailed data shown in the previous section was run for 7 years and the last steps in the model output was compared to the measurements from 6 mbs, 7 years after the injection done for this study. It turned out that the exchangeable cations and the pH were a little off, so the cation exchange capacity (CEC) was increased by 50% from 80 to 120 meq/L of water corresponding to approximately 2 meq/100 g of sediment. The resulting output is shown in Fig. 11. This fit appears to be a reasonable approximation. The CEC is somewhat high compared to other groundwater systems. A high cation exchange capacity will prolong the effects of a leak, so the model is probably a conservative estimate of the prolonged effects in an aquifer without carbonate mineral. The simulated pH is approximately 0.2 units higher than the measured, this could

be an inaccuracy in the model description, but it could also be related to differences in the recharge chemistry or processes occurring upstream.

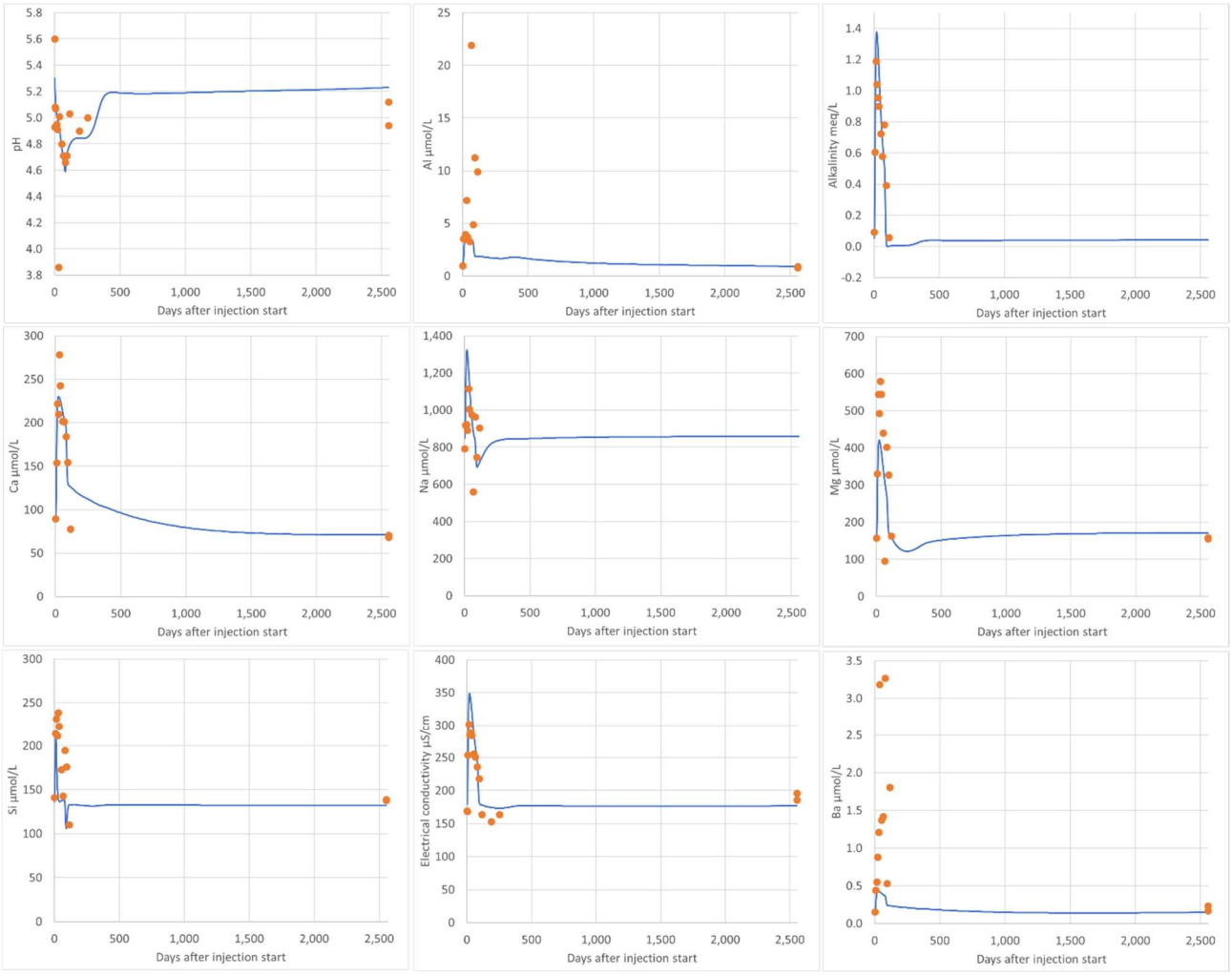

Figure 11: The fit for the model shown in Fig. 9 and 10, run for 7 years with the cation exchange capacity increased by 50% to 120 meq/L (~2 meq/100 g sediment)

4.1.4 Modelled consequences of extended leakage at greater depth

If a leak occurs at greater depth, the P_{CO2} will be higher so lower pH values can be expected. However, going to greater depth might also imply that the sediments will be below the acidification front, so that carbonate minerals will be present. In addition, the lower pH could imply that silicate dissolution would start to play a role. However, silicate dissolution is too insignificant in the injection test carried out to reasonably allow for a fitting of long-term rates of silicate dissolution, so the very small amount of amphibole dissolution to release Ba present in the 7 year model was taken out and substituted by a small amount of kaolinite dissolution. Without dissolution of primary silicates means that using the model as it is, with a higher P_{CO2}, should give a conservative estimate of the effects, because the summed buffering effects of dissolution of a suite of silicate minerals are not included. On the other hand, it also implies that other potential trace elements released from dissolving silicate minerals are not included, but this would most certainly also differ substantially from site to site. In other words if there is a risk of leakage encountering an absolutely carbonate free aquifer at depth, an estimation of the effects on this should include specific tests on the actual sediment addressing the determination of actual dissolution rates and the trace elements that could be released. Nevertheless, to obtain an indication of the pH values that could be expected as well as the possible extent of the resulting plume, the model with the increased CEC used for simulating the 7 year period shown in Fig. 11 was modified using a P_{CO2} of 5 atm, and a duration in the leakage of 1 year. The results for the pH, Al, and EC for the 4000 m

included in the model are shown in Fig. 12 for 3 different times. It appears that the effect of this scenario with high P_{CO2} and a leakage lasting for a full year could affect the groundwater for many years and far downstream of the leakage. Effects are most clear close to the injection at early times and then fade out over time and as the affected water is transported and solutes are dispersed. In this model all of the gibbsite present is dissolved in the part of the aquifer closest to the leakage, implying that to reach a status with gibbsite present would require that gibbsite formed via silicate weathering which could take a very long time. Again, these model results cannot be considered a precise prediction of how the groundwater system will develop after a major leak, primarily due to the exclusion of silicate weathering.

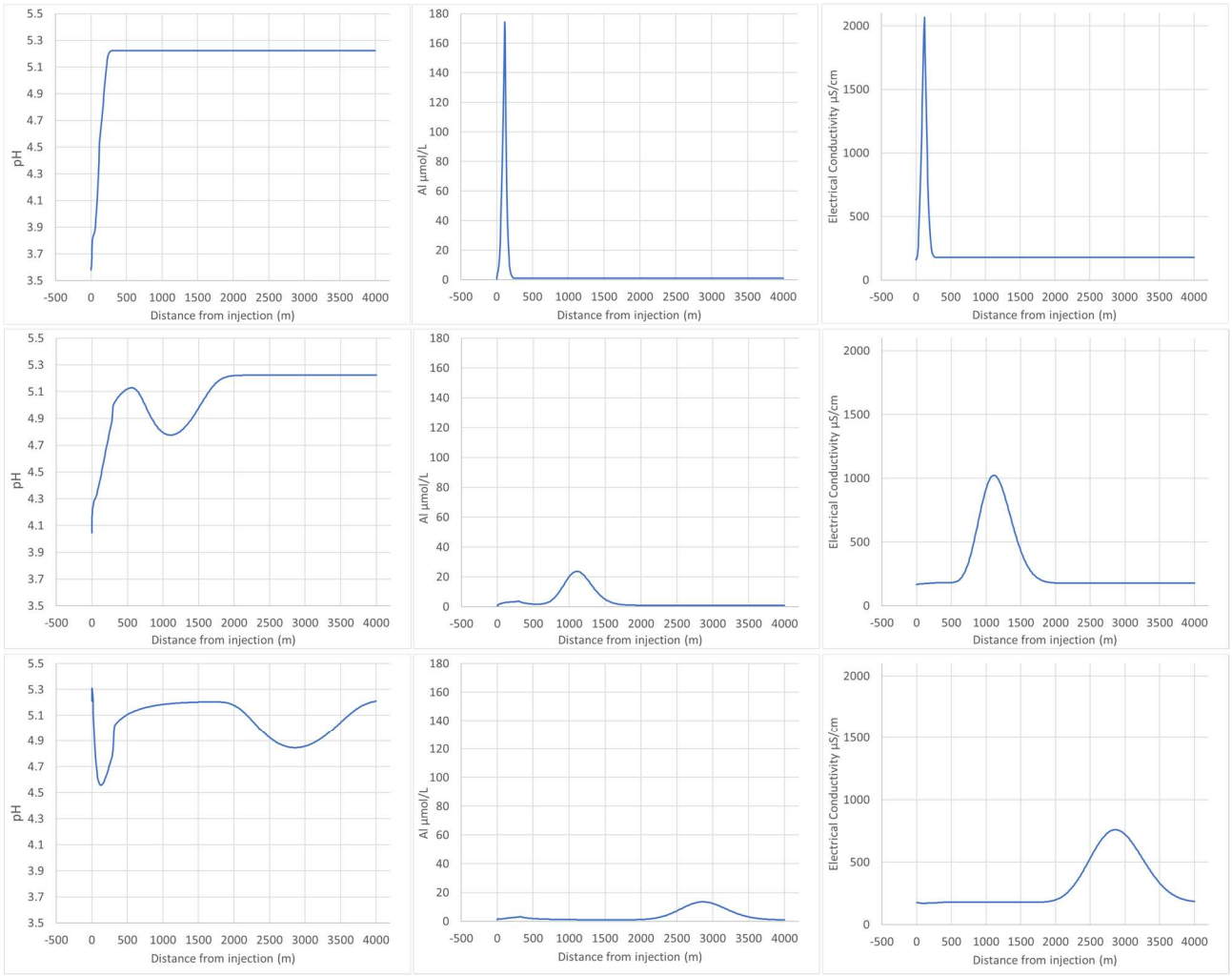

Figure 12: Results from extending the model fitted up to 7 years after the 72 day injection (Fig. 11) to a leakage lasting 1 year at depth, with a PCO_2 of 5 atm.

4.2 CONCEPTUAL SEMIQUANTITATIVE MODEL FOR THE CH_4 INJECTION SITE

Due to the nature of the system and the way the experiment was carried out, where CH_4 appears to be rapidly dispersed within the system as a gas phase migrating ~7 times faster than the groundwater flow, with an unknown amount of CH_4 trapped as bubbles, makes it challenging to set up a reactive transport model. Instead the data are analysed with the aim of picking out significant processes and to the extent it is possible, the rates of these processes and how much CH_4 is oxidized. Since the deeper parts of the system are more affected by the landfill plume, and since the later effects are seen at 2 mbs, the conceptual model and the attempt of quantification relates to the processes as they appear from the data from 2 mbs.

4.2.1 Processes observed during the CH_4 injection experiment and batch modelling

To obtain an estimate of the amount and rate of the oxidation of methane a focus area of the plume around and downstream of the injection that appears to relatively fixed in terms of the distribution of CH_4 was used. The measured water chemistry within the focus area was averaged from day 113 to day 700 and a number of parameters were plotted as a function of time (Fig. 13). Then PHREEQC was used to serially reproduce the average water chemistry in the following averaged set of samples from the focus area using reactions and equilibrium phases and the amounts needed. The reactions included in this modelling are oxidation of methane, equilibrium with calcite, reductive dissolution of Fe-oxides, equilibrium with siderite ($FeCO_3$), reductive dissolution of a Ni-bearing Mn-oxide, precipitation of this due to Mn(II) oxidation and equilibrium with rhodochrosite ($MnCO_3$). The model calculations also included surface complexation using the CD-MUSIC model used in the CO_2 model described above, but here the available surface area was associated to the amount of Fe-oxide in the system implying that when Fe-oxide is reduced relatively more of the trace elements will end up in the water. The PHREEQC input file is shown in Appendix 1. The result of this stepwise model calculation is also shown in Fig. 13.

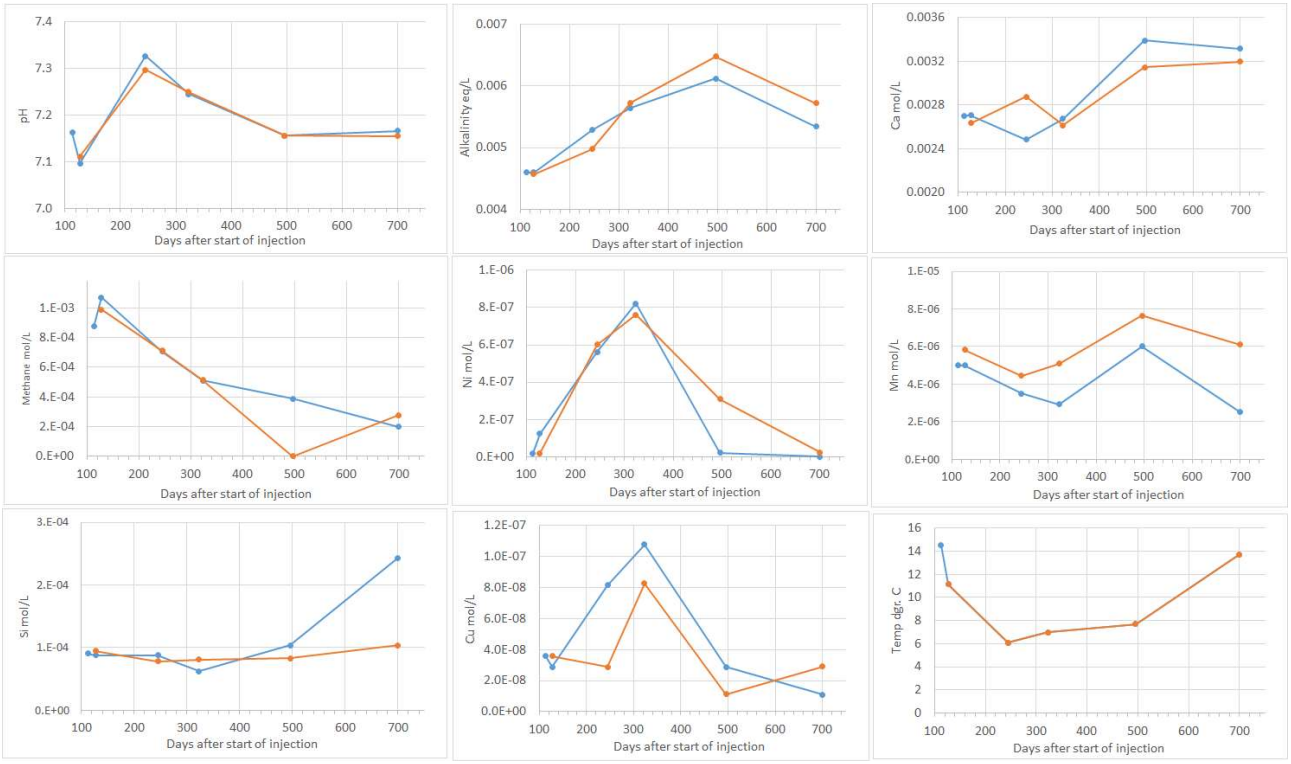

Figure 13: The average chemistry from the focus area (blue) and the results of the stepwise forward modelling done to quantify the amount of occurring processes.

The entirely dominating reactions in the system are the oxidation of CH_4 by O_2 with the simultaneous dissolution of calcite, this was also noted by Cahill et al. (2017) and put together this can be written as:

$$CH_4 + 2O_2 + CaCO_3 => Ca^{2+} + 2HCO_3^- + H_2O \quad (1)$$

implying a 1:1 ratio between oxidized methane and released Ca^{2+} and a 1:2 ratio between the CH_4 consumed and the alkalinity (as HCO_3^-) produced if the process runs to completion. However, the reaction rates of the CH_4 oxidation and the calcite dissolution may not be the same, to take this into account the saturation index for calcite was fixed to the calculated value, thereby controlling the changes in pH and alkalinity. Likewise, the temperature was fixed to the measured temperature to take effects of temperature into account. Fe-oxide reduction via CH_4 oxidation consumes a relatively high amount of acid, even if the Fe^{2+} is precipitated as siderite (Eq. 2).

$$CH_4 + 8FeOOH + 14H^+ => FeCO_3 + 7Fe^{2+} + 13H_2O \quad (2)$$

implying that very little Fe-oxide reduction was needed to produce the increase in pH seen from day 127-245. The Fe-oxide reduction is what gives rise in the variation in the dissolved Cu^{2+}, by desorption and re-adsorption

to the Fe-oxide. Mn-oxide reduction with rhodochrosite precipitation also consumes acid, though the relative amount is smaller:

$$CH_4 + 4MnO_2 + 6H^+ => MnCO_3 + 3Mn^{2+} + 5H_2O \quad (3)$$

The model description of sorption and desorption on Fe-oxides did not affect the Ni concentration, so instead the Mn-oxide reduction was used to produce the observed peak in dissolved Ni^{2+}, assuming that the MnO_2 has a minor amount of Ni(II) in the mineral as an impurity. This also means that when the Mn-oxide reforms, the Ni^{2+} is taken out of solution again. It turned out to be impossible to precipitate enough Mn-oxide to remove all the Ni, and still maintain Mn in solution, this could be due to local variations in the system. However, in terms of the amount of methane oxidized the effect of the Fe- and Mn- oxide reduction is very small and there are presumably alternative ways of explaining the variations in the trace metal concentrations. There is an interesting increase in Si at day 700, which cannot be readily explained. Some of the increase is probably an effect of the higher temperature, but assuming equilibrium with chalcedony (SiO_2), the increase in temperature can only explain a small part of the increase.

The amount of CH_4 oxidized in the different steps in Fig. 13 are tabulated in Table 1, where the amount and fraction of CH_4 calculated to come from trapped methane bubbles is also given and a rate is calculated based on the total amount of methane estimated to have been oxidized.

Table 1: The amounts of methane oxidized and the rate, estimated from the stepwise PHREEQC modelling of the development of the chemistry in the focus area (yellow marking are numbers prior to the indication in Fig. 4 that CH_4 is entering from the side)

	Methane				Total		
Sample day 113	oxidized by reaction mol/L	Initial Solution mol/L	Final Solution mol/L	Reacted solution mol/L	methane oxidized mol/L	fraction from gas	Estimated rate mol/L/d
127	0.00044	0.00087	0.00107	-0.00020	0.00024	1.80	1.74E-05
245	0.00142	0.00107	0.00071	0.00036	0.00178	0.80	1.51E-05
323	0.002	0.00071	0.00051	0.00020	0.00220	0.91	2.82E-05
496	0.00005	0.00051	0.00039	0.00012	0.00017	0.29	9.87E-07
700	0.000016	0.00039	0.00020	0.00019	0.00021	0.08	1.02E-06

The estimated rates derived from the data from day 113 to 323 are relatively close. This is also the period where the CH_4 distribution appears to be less erratic. The rates derived are plotted in Fig. 14 as a function of the methane concentration, the correlation is not very good, and it is not obvious which type of relation there is, so for simplicity a linear relation which goes to zero as the CH_4 concentration goes to zero was chosen. This simple relation is then used in the very simple transport model in order to have a limitation on the rate as the CH_4 is consumed.

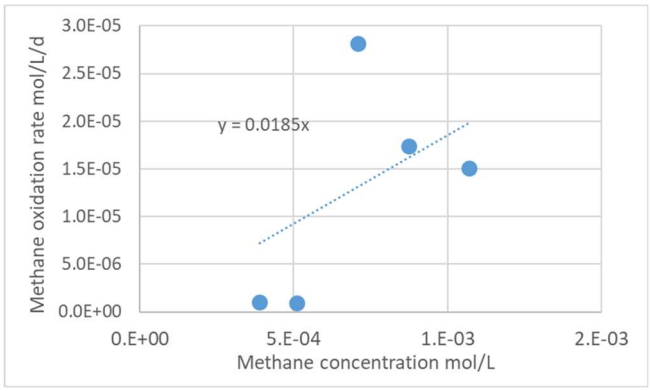

Figure 14: The relation between the methane concentration and the rate of methane oxidation

4.2.2 Simple transport model for the injection experimental period

A simple 1-D PHREEQC transport model is set up, using the rate derived from Fig. 14 and an amount of CH_4 in a gas phase corresponding to the amount of trapped CH_4 gas estimated as having been oxidized (the input file can be seen in Appendix 1). The concentration found to be present in the gas phase was set to be present from -3 to +3 meters on day 113, corresponding to the day of maximum extent. A groundwater velocity of 5 cm/day was used. The resulting 1-D distribution of methane at different timesteps corresponding to the sampling times is shown in Fig. 15. Comparing this with Fig. 4 shows only some resemblance, but due to the very crude simplifications this is to be expected and therefore observations are also not plotted in the diagram.

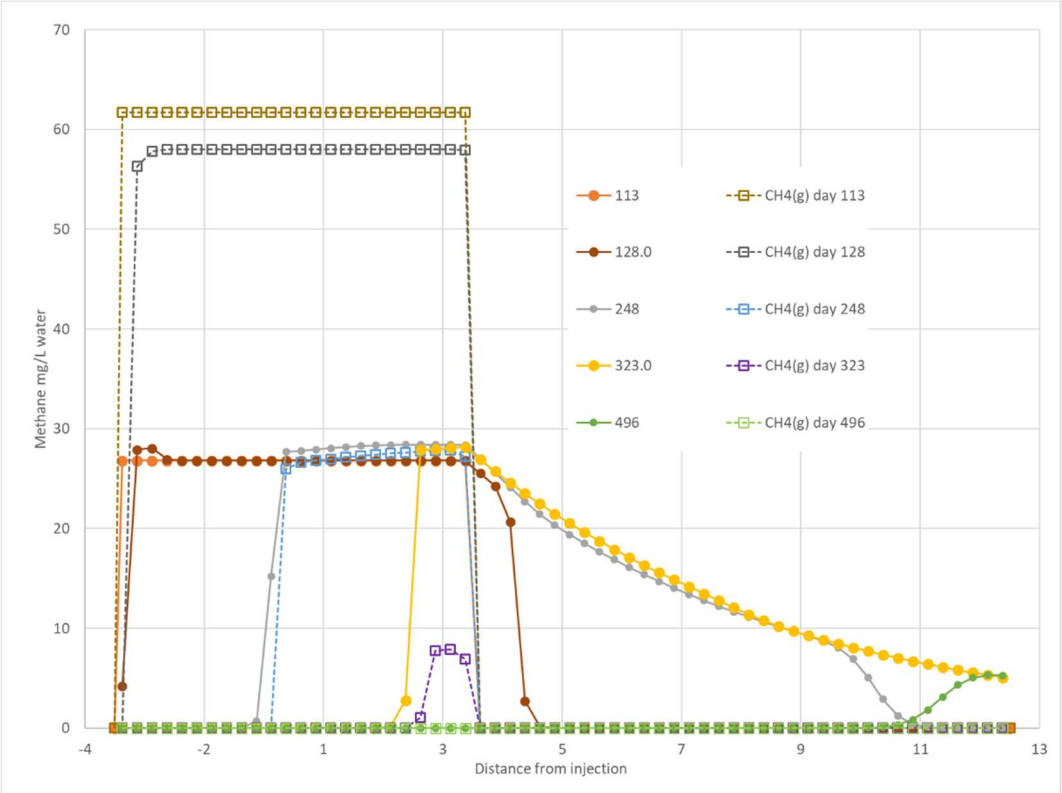

Figure 15: Modelled distribution of methane at the times sampled in a separate gas phase (open squares) and dissolved (filled circles).

The model illustrates how the CH_4 in the gas phase is used up over time while the water is being replaced by the incoming CH_4 free water and the CH_4 in both the gas phase and the water is being used by oxidation. By day 323 very little CH_4 is left in the gas phase. At day 496 the methane is more or less absent from the

monitoring area. This does not resemble the data from day 496, which is thought to be a result of new CH_4 coming in from the side. In the model a high concentration corresponding to the set P_{CH4} is maintained in the cells where there is still CH_4 gas phase left. In the model there is no limit for the availability of O_2 as the amount of CH_4 oxidation is controlled by the amount of CH_4 added by the kinetic expression. Preliminary calculations indicated that a diffusive flux from the water table at around 1 mbs to the sample depth of 2 mbs would be too small to provide enough O_2 indicating that another or additional mechanism must be responsible for providing the O_2. Though pure speculation, it could perhaps be transport via or along plant roots or biopores of some sort? It could also indicate that the oxidant was a solid phase in the sediment, such as Fe- or Mn-oxides, but the calculations carried out above show that the effect on pH would be much too large if a large part of the oxidant was Fe- and Mn-oxides. This was also noted by Forde *et al.* (2019) in their interpretation of the dataset available 700 days after the start of the injection. This indicates that the main oxidant must be O_2, but if O_2 supply is limited downstream or in another setting this would imply that it would take longer to oxidize the CH_4 which would therefore travel longer. Because the CH_4 present at day 496 is probably a result of new methane coming in from adjacent areas, it is not really possible to compare a model result from day 1597 with the samples taken for this report on day 1597. This of course makes further extrapolations uncertain.

4.2.3 Extrapolation of the model to a longer lasting leak

In spite of the uncertainty associated with the model an attempt is made of extrapolating it to a larger leak to obtain an idea of how far a leak may spread under the conditions in this system. The model assumes that it is the injection of 4 m^3/day for the last two days of the injection that gives rise to the plume with a trapped gas phase extending over approximately 6 meters in the aquifer at 2 mbs. Assuming a 100-day leak, this is then simply extended proportionally, forming a plume of trapped CH_4 extending over 300 meters. From this starting point it is assumed that the same groundwater flow rate and CH_4 oxidation rates used in the model presented in the previous section applies. Based on these inputs the model results in the output presented in Fig. 15.

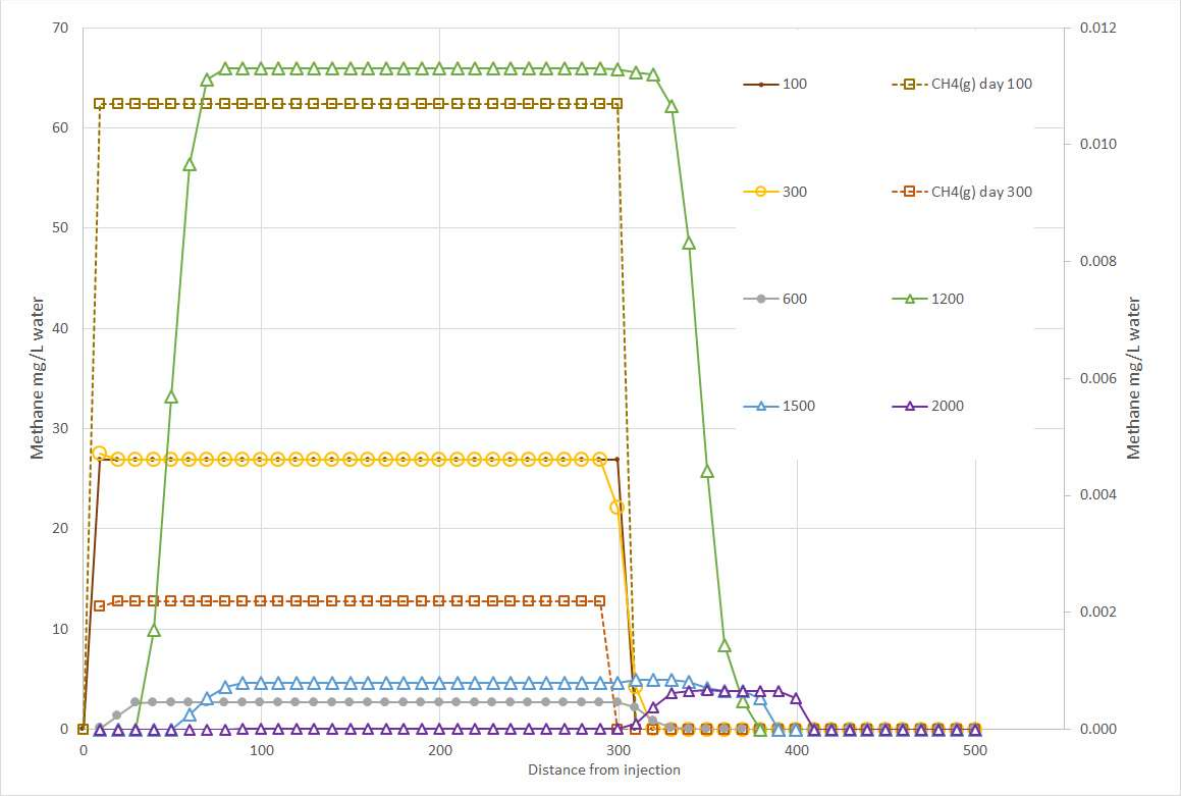

Figure 16: Model based on an extrapolation of the simplified model shown in Fig. 15. Initially 300 m of the system has CH_4 present as a gas phase (open squares) assumed generated by a 100-day leak. The filled circles show the concentration of dissolved CH_4 at different days. To be able to see the concentrations at late times (1200 days and later, open triangles) these are plotted on the secondary Y-axis

As seen in Fig. 16 the CH_4 concentration stays high as long as there is CH_4 gas present, and then declines. After 7 years there are only minor traces <1 µg/L of CH_4, 120 m downstream of the 300 m plume with a CH_4 gas phase. This indicates that when the CH_4 from a leak comes near the surface attenuation by oxidation will limit the extent of spreading from a leak. If the CH_4 is transported in an anaerobic, naturally methanogenic groundwater system there will not be any oxidation and the CH_4 would travel as an inert compound with the groundwater until it came into contact with an oxidizing environment.

5 Discussion

5.1 IMPLICATIONS FOR THE RISK TO AQUIFERS ASSOCIATED WITH CO_2 STORAGE

The experiment carried out in the Vrøgum plantation indicates that effects on groundwater quality of relatively short leaks (months) are limited as already reported by (Cahill, Marker and Jakobsen, 2014). Short term leaks could be leaks occurring due to failed infrastructure, e.g. injection or monitoring wells. Because the possible location is known to be along a specific well, the chances of closing it off or sealing the leak within a relatively short timeframe are high, implying that a relatively short leak is realistic. Leaks related to the geology of the system may have gone unnoticed for some time, will be more difficult to locate precisely and may be larger. The nature and size of the leak may make a direct sealing of the leak difficult making it more probable that the leak will be stopped by changing in the pressure distribution of the system. There is a successful example summarized by Benson and Hepple (2005) for the gas storage in Galesville, IL, USA that leaked into a groundwater reservoir above it. Here it was possible to stop the leakage by reducing the pressure below the leak and increasing it above. Operations like this could take some time and all these different factors imply that leaks related to the geology will probably be longer lasting leaks than leaks related to infrastructure.

The effects of longer lasting leaks entering into aquifers at greater depths were assessed using an extension of the model modified to better fit the observations made 7 years after the short-term injection. The leak was extended to last for 1 year. According to the model, effects in the form of a lower pH down to around a pH of 3 could be expected. Due to the lack of carbonates a low pH, though increasing slowly downstream, did not completely reach the background pH value within 4000 m downstream of the leak after 100 years, but it came close and effects will decrease downstream due to dispersion. This should be considered a conservative estimate of the extent and duration of a 1-year leak since the model did not include buffering effects of silicate mineral dissolution. The rate of silicate dissolution increases dramatically as pH is lowered, so silicate mineral dissolution would have an effect. The actual resulting extent and duration would therefore be smaller. However, the silicate weathering could release concentrations of trace elements, though sorption to Fe- and Mn-oxides, that would also be produced by the silicate weathering, would lead to a retardation of the released trace elements, and since the silicate weathering would stop when the pH increases again, the effect of the sorption would be a longer lasting but lower concentration of trace elements further downstream. In terms of possible effects on ground water quality for a downstream water supply, the effects are of a nature and a magnitude that can be treated at the water works before the water is sent out to consumers. This may require new infrastructure at the water works, implying that monitoring should be frequent enough to give notification early enough for new infrastructure to be installed before the plume arrives. Depending on the situation it may also be possible to address the plume within the aquifer using techniques used in the environmental industry for other pollution plumes such as pump'n'treat, or injection of reactants into the aquifer.

5.2 IMPLICATIONS FOR THE RISK TO AQUIFERS ASSOCIATED WITH UNCONVENTIONAL CH_4

Data from the injection experiment indicate that due to the low solubility of CH_4 the CH_4 may be trapped as a gas phase in the sediment for extended periods maintaining a high concentration in the water flowing through the aquifer. If the CH_4 is trapped near the water table, it appears that there is a high chance of a natural attenuation of the CH_4 by oxidation with atmospheric oxygen. This will limit the extent of a plume and the concentrations in the water. Due to the complexity of the data it is difficult to predict how efficient the oxidation of CH_4 will be at another site. The flux of O_2 to the CH_4 is obviously very important, but based on the available data it has not been possible to clarify how the O_2 is transported to the CH_4 at 2 mbs in the studied system.

In the other extreme, the CH_4 spreading in a highly reduced methanogenic aquifer where the CH_4 added from a leak will be inert, except at very high pressures (e.g., ~80 bar) where acetate formation from CH_4 may occur (Yang *et al.*, 2020). Since this is higher than the pressure in most fresh water aquifers used for drinking water,

the CH_4 in a methanogenic aquifer used for drinking water will travel as far the aquifer is methanogenic and presumably some distance into a system containing oxidants. In between the two extremes (oxic and methanogenic) there should eventually develop domains of anaerobic methane oxidation. This can be driven by the dissolved oxidants nitrate and sulphate (sulphate could also be present as gypsum) or mineral phases such as Fe- and Mn-oxides. For the dissolved oxidants the efficiency will depend on the extent of mixing between water with CH_4 and water with oxidant. For the mineral phases it will depend on the reactivity of the minerals. In all cases there could be a lag phase before a significant population of methanotrophic microorganisms is established. In the case of reduction of Fe- and Mn-oxides this could result in the release of trace metals as indicated at the studied site, but also seen for arsenic (As) released from Fe-oxides in the aquifers of SE Asia (e.g. Postma *et al.*, 2016) or Ni released from Mn-oxides (e.g. Larsen and Postma, 1997). Both high CH_4 concentrations and trace metal concentrations can be dealt with using techniques already used at water works. The CH_4 can be stripped by vigorous aeration and trace metals can be sorbed to Fe-oxides formed already, or if the amounts are insufficient they can be produced (e.g. van Genuchten *et al.*, 2020) as part of the water treatment.

5.3 IMPLICATIONS FOR WHY AND HOW THIS WORK IS RELEVANT FOR INDUSTRY

Both examples show that the effects of a leakage and the duration of the effects, not surprisingly, relate to the duration of the leakage, implying that early detection of leakage as well as rapid closure of the leakage will lower the impact of any leakage that might occur. The results also show that the effects caused by leakage may lead to a water quality that will need to be treated, however the effects are of a type and a magnitude that can be treated using existing relatively simple water treatment technologies already used at some water works. Though treatment is possible, the treatment will imply extra costs for building the treatment systems as well as increased running costs for the water production. The running costs will of course depend on the time frame for which they are needed, underlining that one should aim for early detection, which will be a function of the monitoring program, and rapid closure of a leak which will depend on detailed knowledge of the geology, pressure distribution, flows, etc. of the site making it possible to perform a rapid remediation.

5.4 RECOMMENDATIONS FOR THE RISK ASSESSMENT OF DETRIMENTAL EFFECTS ON GROUNDWATER QUALITY IN POSSIBLY AFFECTED AQUIFERS

Leakage into an aquifer of CO_2 or CH_4 implies both a direct risk associated with the CO_2 or CH_4 and a derived risk caused by reaction products generated when the CO_2 or CH_4 reacts with the water and the minerals present in the aquifer. The risk associated with the gases themselves is small as long as they stay in the groundwater, but may cause severe problems when they reach the surface where they may lead to suffocation or explosions, this is considered outside the frames of this study. CO_2 will dissolve in the groundwater and produce carbonic acid and the acidic water will cause dissolution of minerals which will release the ions held in the minerals, both the major constituents, but also trace elements which may be harmful. CH_4 is a reduced compound implying that it may lead to reductive dissolution of Fe- and Mn-oxides as well as reduction of dissolved or mineral bound (gypsum) sulfate, producing H_2S. What minerals are dissolved depends on both their presence, amounts and reactivities and cannot be predicted, implying that it is necessary to do experiments with the actual aquifer material to assess the risk associated with a leak. Tests on the reactions with aquifer materials may be performed in the lab or in the aquifer itself, though both is preferable to cover a range of pressure conditions and leakage durations and aid in extrapolating to *in-situ* conditions. Based on tests, modelling of the tests and extrapolations from these, the elements and compounds released, their concentrations and relative transport velocities can be assessed. In addition to knowledge of the chemistry that may develop in case of leakage it is also necessary to know the aquifer flow system that will transport the possible contamination towards streams and surface waters as well as water works. Putting this together in a reactive transport model and combining it with a range of leakage scenarios should allow an assessment of the risk associated with different leakage scenarios. The risk assessment should include an assessment of the risk that the contamination cannot be treated and if this is the case, how long the situation will likely last.

Appendix 1

This appendix holds the input files used for the modelling. For the modelling of the CO_2 site there is a set of files for PHAST, consisting of the transport file and the geochemistry file for the 7 year model the long term model was identical except that the model was extended to 250 m and the simulation time was 48 years. Finally, the CD-MUSIC model part of the database file, based on the wateqf.dat file included with PHREEQC, used in both simulations is listed. For the CH_4 injection experiment the PHREEQC files include the file with forward models used to estimate the amount of CH_4 oxidized and the rate, the transport model for the attenuation of the CH_4 in the injection experiment and the model extending this to the attenuation of a 100-day leak.

PHAST MODEL USED FOR MODELLING THE CO_2 SITE

7 year model – transport file and chemistry file

```
PHAST transport file
TITLE
.       CO2 INJECTION 7 YEARS
SOLUTE_TRANSPORT true
      -diffusivity  1e-009
STEADY_FLOW true
      -head_tolerance 1e-012
      -flow_balance_tolerance 1e-012
      -iterations 10000
      -growth_factor 1.05
FREE_SURFACE_BC false
SOLUTION_METHOD
      -iterative_solver   false
      -space_differencing 0
      -time_differencing  1
      -cross_dispersion   false
      -rebalance_fraction 0
      -rebalance_by_cell  true
UNITS
      -time                              days
      -horizontal_grid                 m
      -vertical_grid                 m
      -map_horizontal                m
      -map_vertical                    m
      -head                              m
      -hydraulic_conductivity          m/s
      -specific_storage                1/m
      -dispersivity                    m
      -flux                            meters/day
      -leaky_hydraulic_conductivity    m/s
      -leaky_thickness                 m
      -well_diameter                   m
      -well_flow_rate                  m^3/s
      -well_depth                      m
      -river_bed_hydraulic_conductivity m/s
      -river_bed_thickness             m
      -river_width                     m
      -river_depth                     m
      -drain_hydraulic_conductivity    m/s
      -drain_thickness                 m
      -drain_width                     m
      -equilibrium_phases        WATER
      -exchange                        WATER
      -surface                           WATER
      -solid_solutions                 WATER
      -kinetics                          WATER
      -gas_phase                       WATER
GRID
      -nonuniform X
            0    0.25    0.5    0.75    1
            1.25    1.5    1.75    2    2.25
            2.5    2.75    3    3.25    3.5
            3.75    4    4.25    4.5    4.75
            5    5.5    6    6.5    7
            7.5    8    8.5    9    9.5
            10    10.5    11    11.5    12
            12.5    13    13.5    14    14.5
            15    15.5    16    16.5    17
            17.5    18    18.5    19    19.5
            20    21    22    23    24
```

```
            25    26    27    28    29
            30
      -uniform Y 0 1 2
      -uniform Z 0 1 2
      -snap X 0.001
      -snap Y 0.001
      -snap Z 0.001
      -chemistry_dimensions X
      -print_orientation XY
      -grid_origin   0  0  0
      -grid_angle    0
MEDIA
      -domain
            -active                   1
            -Kx                       0.00023
            -Ky                       0.00023
            -Kz                       0.00023
            -porosity                 0.3
            -specific_storage         1
            -long_dispersivity        0
            -horizontal_dispersivity  0
            -vertical_dispersivity    0
            -tortuosity               1
FLUX_BC
      -box 0 0 0 0 1 1 GRID
            -description Influx m/day
            -face X
            -associated_solution
                  0 years     1
                  0.21 years  2
            -flux
                  0 years     2
            #due to a bug this does not correspond
            #to the flow rate (0.16 m/d) but was fitted
FLUX_BC
      -box 30 0 0 30 1 1 GRID
            -description Outflux m/day
            -face X
            -associated_solution
                  0 years     2
            -flux
                  0 years     2
            #same value as influx
HEAD_IC
      -domain
            -head                     X 10 0 9.92 30
CHEMISTRY_IC
      -domain
            -description InitialChemistry
            -solution             2
            -equilibrium_phases   2
            -exchange             2
            -surface              2
            -kinetics             2
PRINT_INITIAL
      -boundary_conditions        false
      -components                 false
      -conductances               false
      -echo_input                 false
      -fluid_properties           false
      -force_chemistry_print      false
      -HDF_chemistry              true
      -HDF_heads                  true
      -HDF_media                  true
      -HDF_steady_flow_velocities true
      -heads                      false
      -media_properties           false
      -solution_method            false
      -steady_flow_velocities     false
      -wells                      false
      -xyz_chemistry              true
      -xyz_components             false
      -xyz_heads                  false
      -xyz_steady_flow_velocities false
      -xyz_wells                  false
PRINT_FREQUENCY
      -save_final_heads true
      0
            -bc_flow_rates          0
            -boundary_conditions    false
            -components             0
            -conductances           0
            -end_of_period_default  true
            -flow_balance           end
            -force_chemistry_print  0
```

```
      -HDF_chemistry          1    days
      -HDF_heads              end
      -HDF_velocities         0
      -heads                  end
      -progress_statistics    100    days
      -restart_file           0
      -velocities             0
      -wells                  end
      -xyz_chemistry          3    days
      -xyz_components         0
      -xyz_heads              0
      -xyz_velocities         0
      -xyz_wells              0
      -zone_flow              end
      -zone_flow_xyzt         end
      -zone_flow_tsv          end
      -hdf_intermediate       100    days
730
      -bc_flow_rates          0
      -boundary_conditions    false
      -components             0
      -conductances           0
      -end_of_period_default  true
      -flow_balance           end
      -force_chemistry_print  0
      -HDF_chemistry          5    years
      -HDF_heads              end
      -HDF_velocities         0
      -heads                  end
      -progress_statistics    5    years
      -restart_file           0
      -velocities             0
      -wells                  end
      -xyz_chemistry          30    days
      -xyz_components         0
      -xyz_heads              0
      -xyz_velocities         0
      -xyz_wells              0
      -zone_flow              end
      -zone_flow_xyzt         end
      -zone_flow_tsv          end
      -hdf_intermediate       end
365 days
      -bc_flow_rates          0
      -boundary_conditions    false
      -components             0
      -conductances           0
      -end_of_period_default  true
      -flow_balance           end
      -force_chemistry_print  0
      -HDF_chemistry          1    days
      -HDF_heads              end
      -HDF_velocities         0
      -heads                  end
      -progress_statistics    1    years
      -restart_file           0
      -velocities             0
      -wells                  end
      -xyz_chemistry          15    days
      -xyz_components         0
      -xyz_heads              0
      -xyz_velocities         0
      -xyz_wells              0
      -zone_flow              end
      -zone_flow_xyzt         end
      -zone_flow_tsv          end
      -hdf_intermediate       2    years
3 years
      -bc_flow_rates          0
      -boundary_conditions    false
      -components             0
      -conductances           0
      -end_of_period_default  true
      -flow_balance           end
      -force_chemistry_print  0
      -HDF_chemistry          0.05    years
      -HDF_heads              end
      -HDF_velocities         0
      -heads                  end
      -progress_statistics    5    years
      -restart_file           0
      -velocities             0
      -wells                  end
      -xyz_chemistry          30    days
      -xyz_components         0
```

```
            -xyz_heads              0
            -xyz_velocities         0
            -xyz_wells              0
            -zone_flow              end
            -zone_flow_xyzt         end
            -zone_flow_tsv          end
            -hdf_intermediate       1    years
TIME_CONTROL
      -time_step
            0 0.02 days
            0.4 0.05 days
      -time_change
            2555 days
      -start_time 0 days
```

PHAST chemistry file

```
#DATABASE C:\Program Files (x86)\USGS\Phreeqc Interactive 3.6.2-15100\database\cdm_jessenetal2012.dat
## 1D reactive transport model of controlled CO2 release, Vrøgum aquifer
## Rasmus Jakobsen - Palandri and Kharaka kinetics added Modified from A.Cahill version (modified
from P. Marker, August 2012)
## use cdm_jessenetal2012.dat database

SELECTED_OUTPUT
-file  AP_Kin1.xls
-state false
-user_punch true
-simulation true
-solution true
-distance true
-time true
-step true
-ph true
-alkalinity true
-pe false
-ionic_strength true
-charge_balance true
-percent_error true
-totals Ca Mg Na K Al Si Fe Mn Ba Cu Ni Sr Zn Br
-molalities CaX2 MgX2 NaX KX AlX3 SrX2 BaX2 ZnX2 HX
-saturation_indices CO2(g) Gibbsite KGibbsite Al(OH)3(a) Kaolinite Chalcedony Montmorillonite-Ca \
Ba-Amphibole Pyroxene
-equilibrium_phases gibbsite Al(OH)3(a) Fe(OH)3(a) Kaolinite
-kinetic_reactants Gibbsite Ba-Amphibole Ba-mica Pyroxene KGibbsite KKaolinite

# The CEC (total based on Ca, Mg, K, Na, Al and NH4+) has been determined  in the
# laboratory. The CEC was determined on two sediment samples from eight meters
# depth (double determination). The results were very similar. By comparing the measured
# exchanger composition of Ca, Mg, K, Na, Al, NH4+, Ba, Sr and Zn with that suggested
# by phreeqc, the log_k distribution coeffcients have been fitted to match
# the measured distribution.

EXCHANGE_SPECIES

      Na+ + X- = NaX
      log_k   0
      -gamma      4.0  0.075

    Mg+2 + 2X- = MgX2
      log_k -0.83
      -gamma      5.5   0.2
      delta_h  7.4      # Laudelout et al., 1968

      Ca+2 + 2X- = CaX2
      log_k   0.45
      -gamma      5.0   0.165
      delta_h  7.2      # Van Bladel & Gheyl, 1980

      K+ + X- = KX
      log_k 0.8
      -gamma      3.5   0.015
      delta_h  -4.3     # Jardine & Sparks, 1984

      Al+3 + 3X- = AlX3
      log_k -0.1
      -gamma      9.0   0.0

      Ba+2 + 2X- = BaX2
      log_k   0.25
      -gamma      5.0   0.0
      delta_h  4.5      # Laudelout et al., 1968

        Sr+2 + 2X- = SrX2
```

```
      log_k -0.5
      -gamma      5.26  0.121
      delta_h  5.5      # Laudelout et al., 1968

      Zn+2 + 2X- = ZnX2
      log_k -0.35
      -gamma      5.0   0.0

PHASES #Amphibole and Pyroxene From P. Markers model (amphibole changed from 0.5Ba to 0.05Ba
Ba-Amphibole # Assumed Ba-bearing hornblende, also releasing Al, Fe, Ca, Si and Mg  med ind...
      Ba0.05Ca1.95Mg4.94Fe0.02Al0.02Si8O22(OH)2 + 14H+ + 8H2O = 0.05Ba+2 + 1.95Ca+2 + 4.94Mg+2 +
0.02Fe+3 + 0.02Al+3 + 8H4SiO4
      log_k       56.574
      delta_h -96.853 kcal
#Kinetic gibbsite - with a slightly cahanged log_k
KGibbsite         51
      Al(OH)3 + 3H+ = Al+3 + 3H2O
      log_k       8.20  #Increased by 0.09 to give slightly more unstable gibbsite - higher Al
      delta_h -22.8 kcal

Ba-mica           43
      K0.95Ba0.05Al3.05Si2.95O10(OH)2 + 10.2H+ = 0.95K+ + 0.05Ba+2 + 3.05Al+3 + 2.95H4SiO4 +0.2H2O
      log_k       12.703
      delta_h -59.376 kcal

KKaolinite        46
      Al2Si2O5(OH)4 + 6H+ = 2Al+3 + 2H4SiO4 + H2O
      log_k       8.725      #raised by 1.29 for more stable Kaolinite corresponding to measured \
background where SI=1.29
      delta_h -35.3 kcal

# average background
SOLUTION  0
units mmol/l;temp 8;pH  5.46;redox O(-2)/O(0)
Alkalinity 0.078; O(0) 0.422;Cl 0.943;N(+5) 0.020;S(6) 0.160;P   0.0009;N(+3) 0.00036 #N(-3) 0.0040 \
Al    0.0013;Ba   0.00017;Ca  0.091;Fe 0.002;K 0.0597;Mg    0.168;Mn 0.00326;Si     0.129;Na 0.857 \
Sr    0.000485; Zn 2.5E-04; Br 1.0E-3

EQUILIBRIUM_PHASES  0
CO2(g) -0.15
SAVE solution 1
END
#_____________________________________________________________________________________________
#
#USE solution 0

SOLUTION 2
units mmol/l;temp 8;pH  5.46;redox O(-2)/O(0)
Alkalinity 0.078;O(0) 0.422;Cl 0.943;N(+5) 0.020;S(6) 0.160;P    0.0009;N(+3) 0.00036 #N(-3) 0.0040 \
Al    0.0013;Ba   0.00017;Ca  0.091;Fe 0.002;K 0.0597;Mg    0.168;Mn 0.00326;Si     0.129;Na 0.857 \
Sr    0.000485;Zn 2.5E-04

EXCHANGE  2
X 120e-03
-equilibrate 2

SURFACE  2  # goethite's surface #From P. Marker model
Goe_uniOH-0.5 4.9 60 17.58    #surface increased to 140%  3.5 -> 4.9 & 2.8 -> 3.92
Goe_triOH-0.5 3.92
-cd_music
-sites_units density
-equilibrate 2

SAVE solution 2

END


KINETICS 2
Ba-Amphibole
-m0 0.1
#hornblende -7.00 75.5 0.600        -10.30 94.4 **Parameters from Palandri and Kharaka, 2004
#     Acid:  alogk  bE  cn  neutral: alogk  bE
# non logform: 1e-7  75.5    0.600         5.012e-11  94.4
-parms 0.1 1.0    1.0e-7 75.5 0.6          5.012e-11 94.4
#      Area Vol   k     bE  cn   neutral:  k        bE
-tol  1e-12
#-step_divide 0.1
-cvode true
-cvode_order 5
-cvode_steps 1000
-bad_step_max 50000

#
Kgibbsite
```

```
-m0  0.002
#gibbsite  -7.65 47.5 0.992         -11.50 61.2        -16.65 80.1 -0.784 **Parameters from Palandri
and Kharaka, 2004
#   id:   alogk  bE  cn   neutr:   alogk  bE   alk:    alogk  bE   cn
-parms   4800   1      2.239E-8   47.5 0.992        3.162E-12  61.2    2.239E-17 80.1 -0.784
#       Area Vol acid: k         bE    cn  neutr:   alogk  bE      alk:  k      bE     cn
-tol  1e-12
#-step_divide 0.1
-cvode true
-cvode_steps 1000
-cvode_order 5
-bad_step_max 50000

RATES
Ba-Amphibole  #Ba-bearing hornblende
 -start
      # Parameters from Palandri and Kharaka, 2004
      # parm(1) = A in m2; parm(2) = V in L (recalc's sp. rate to mol/kgw)
      # parm(3) = k25, acid(rate const. at 25 C); parm(4) = Ea, acid;
      # parm(5) = n, acid;
      # parm(6) = k25, neutral; parm(7) = Ea, neutral;
      ## parm(8) = k25, carb; parm(9) = Ea, carb; parm(10) = m, carb;
      ## parm (11) = k25, alk; parm(12) = Ea, alk; parm(13) = n, alk
 1  A0 = parm(1) #
 2  V = parm(2)  #1
 3  k25ac = parm(3) #1e-7
 4  Eaac = parm(4) #75.5
 5  nac = parm(5) #0.6
 6  k25n = parm(6) #5.12e-11
 7  Ean = parm(7) #94.4
 #8  k25c = parm(8) #0.0 - due to lack of data for this part of the rate expressions
 #9  Eac = parm(9) #0.0
 #10 nc = parm(10) #0.0
 #11 k25al = parm(11) #0.0
 #12 Eaal = parm(12) #0.0
 #13 nal = parm(13) #0.0

 20 dif_T = (1/TK) - (1/298.15) # temp corrected with the Arrhenius eqn.
           # the difference in temperature, TK gives solution temp in Kelvin...
                       # rate by neutral
 22 r_neut = k25n*exp((-Ean*1000/8.314472)*dif_T)
                       # rate by H+...
 24 r_acid = k25ac*(exp((-Eaac*1000/8.314472)*dif_T))*((act("H+"))^nac)
                       # rate by OH-....
 # 26 r_alk = k25al*(exp((-Eaal*1000/8.314472)*dif_T))*((act("H+"))^nal) #no alkaline rate parameters
                       # Sum the rate contributions...
 60 rate = r_neut + r_acid # + r_alk   #no alkaline rate parameters
                       # normalize to mol/kgw, correct for m/m0 and the approach to equi...
 70 rate = rate * (A0 / 0.3) * ((m/m0)^0.67) * (1 - SR("Ba-Amphibole"))
      #divided by 0.3 instead of V=1 to transform to PHAST #power 2 instead of 0.67
      # integrate...
 80 moles = rate * time
 90 save moles
 -end


KGibbsite
-start
     # Parameters from Palandri and Kharaka, 2004
     # parm(1) = A in m2; parm(2) = V in L (recalc's sp. rate to mol/kgw)
      # parm(3) = k25, acid(rate const. at 25 C); parm(4) = Ea, acid;
      # parm(5) = n, acid;
      # parm(6) = k25, neutral; parm(7) = Ea, neutral;
      ## parm(8) = k25, carb; parm(9) = Ea, carb; parm(10) = m, carb;
      ## parm (11) = k25, alk; parm(12) = Ea, alk; parm(13) = n, alk
 1  A0 = parm(1)
 2  V = parm(2)
 3  k25ac = parm(3)
 4  Eaac = parm(4)
 5  nac = parm(5)
 6  k25n = parm(6)
 7  Ean = parm(7)
 #8  k25c = parm(8) #0.0 - due to lack of data for this part of the rate expressions
 #9  Eac = parm(9) #0.0
 #10 nc = parm(10) #0.0
 11 k25al = parm(8)
 12 Eaal = parm(9)
 13 nal = parm(10)
                       # temp corrected with the Arrhenius eqn.
                       # the difference in temperature, TK gives solution temp in Kelvin...
 20 dif_T = (1/TK) - (1/298.15)
           # rate by neutral
 22 r_neut = k25n*exp((-Ean*1000/8.314472)*dif_T)
           # rate by H+...
 24 r_acid = k25ac*(exp((-Eaac*1000/8.314472)*dif_T))*((act("H+"))^nac)
```

```
          # rate by OH-....
  26 r_alk = k25al*(exp((-Eaal*1000/8.314472)*dif_T))*((act("H+"))^nal)
          # Sum the rate contributions...
 60 rate = r_neut + r_acid + r_alk
                    # normalize to mol/kgw, correct for m/m0 and the approach to equi...
 70 rate = rate * (A0 / 0.3) * ((m/m0)^2.5) * (1 - SR("KGibbsite"))  #DIVIDED BY 0.3 instead of V=1
 #to transform to PHAST #power 2.5 instead of 0.67
                    # integrate...
 80 moles = rate * time
 90 save moles
 -end
```

PART OF DATABASE FILE USED FOR BOTH THE CO2 MODELS ONLY PARTS THAT DIFFER FROM THE STANDARD wateqf.dat file included with PHREEQC is listed

```
# Part of Database file used by Jessen et al. (2012) for CD MUSIC modeling in PHREEQC.
# the rest of the file is $Id: wateq4f.dat 431 2005-08-23 17:29:36Z dlpark $
# apart from Arsenic data from Archer and Nordstrom (2002)
# they have been replaced by those of Langmuir et al. (2006).
# CD music parameters of Table EA-1 in Jessen et al. (2012).

#H2AsO3-           478      from Langmuir etal 06 GCA
      H3AsO3 = H2AsO3- + H+
      log_k -9.23  #-9.15
      delta_h     27.45 kJ  #27.54  kJ

#HAsO3-2           479      from Langmuir etal 06 GCA
      H3AsO3 = HAsO3-2 + 2H+
      log_k -21.33 #-23.85
      delta_h     59.41 kJ

#AsO3-3            480         from Langmuir etal 06 GCA
      H3AsO3 = AsO3-3 + 3H+
      log_k -34.74 #-39.55
      delta_h     85.8 kJ #84.73    kJ

#H4AsO3+           481         from Langmuir etal 06 GCA
      H3AsO3 + H+ = H4AsO3+
      log_k -0.29 #-0.305

#H2AsO4-           482   from Langmuir etal 06 GCA
      H3AsO4 = H2AsO4- + H+
      log_k -2.24 #-2.3
      delta_h     -7.11 kJ #-7.066  kJ

#HAsO4-2           483  from Langmuir etal 06 GCA
      H3AsO4 = HAsO4-2 + 2H+
      log_k -9.20 #-9.46
      delta_h     -3.77 kJ #-3.846  kJ

#AsO43-            484  from Langmuir etal 06 GCA
      H3AsO4 = AsO4-3 + 3H+
      log_k -20.7 #-21.11
      delta_h     14.354      kJ

#CaH2AsO4+  from Langmuir etal 06 GCA
      Ca+2 + H3AsO4 = CaH2AsO4+ + H+
      log_k -1.18

#CaHAsO4   from Langmuir etal 06 GCA
      Ca+2 + H3AsO4 = CaHAsO4 + 2H+
      log_k -6.51

#CaAsO4-   from Langmuir etal 06 GCA
      Ca+2 + H3AsO4 = CaAsO4- + 3H+
      log_k -14.48
#MgH2AsO4+  from Langmuir etal 06 GCA
      Mg+2 + H3AsO4 = MgH2AsO4+ + H+
      log_k -0.72

#MgHAsO4   from Langmuir etal 06 GCA
      Mg+2 + H3AsO4 = MgHAsO4 + 2H+
      log_k -6.34

#MgAsO4-   from Langmuir etal 06 GCA
      Mg+2 + H3AsO4 = MgAsO4- + 3H+
      log_k -14.36
#FeH2AsO4+2  from Langmuir etal 06 GCA
      Fe+3 + H3AsO4 = FeH2AsO4+2 + H+
      log_k 1.8

#FeHAsO4+   from Langmuir etal 06 GCA
      Fe+3 + H3AsO4 = FeHAsO4+ + 2H+
      log_k 0.66
```

```
#FeAsO4   from Langmuir etal 06 GCA
      Fe+3 + H3AsO4 = FeAsO4 + 3H+
      log_k -1.8

#FeH2AsO4+  from Langmuir etal 06 GCA
      Fe+2 + H3AsO4 = FeH2AsO4+ + H+
      log_k 0.44

#FeHAsO4   from Langmuir etal 06 GCA
      Fe+2 + H3AsO4 = FeHAsO4 + 2H+
      log_k -5.66

#FeAsO4-   from Langmuir etal 06 GCA
      Fe+2 + H3AsO4 = FeAsO4- + 3H+
      log_k -13.64

#MnHAsO4   from Langmuir etal 06 GCA
      Mn+2 + H3AsO4 = MnHAsO4 + 2H+
      log_k -5.45

#MnAsO4-   from Langmuir etal 06 GCA
      Mn+2 + H3AsO4 = MnAsO4- + 3H+
      log_k -14.57

#NiH2AsO4+  from Langmuir etal 06 GCA
      Ni+2 + H3AsO4 = NiH2AsO4+ + H+
      log_k -0.72

#NiHAsO4   from Langmuir etal 06 GCA
      Ni+2 + H3AsO4 = NiHAsO4 + 2H+
      log_k -6.30

#NiAsO4-   from Langmuir etal 06 GCA
      Ni+2 + H3AsO4 = NiAsO4- + 3H+
      log_k -14.36

#CuHAsO4   from Langmuir etal 06 GCA
      Cu+2 + H3AsO4 = CuHAsO4 + 2H+
      log_k -5.52

#ZnHAsO4   from Langmuir etal 06 GCA
      Zn+2 + H3AsO4 = ZnHAsO4 + 2H+
      log_k -5.99

#CdHAsO4   from Langmuir etal 06 GCA
      Cd+2 + H3AsO4 = CdHAsO4 + 2H+
      log_k -5.49

#PbH2AsO4+  from Langmuir etal 06 GCA
      Pb+2 + H3AsO4 = PbH2AsO4+ + H+
      log_k -0.71

#PbHAsO4   from Langmuir etal 06 GCA
      Pb+2 + H3AsO4 = PbHAsO4 + 2H+
      log_k -6.16

#AlH2AsO4+2  from Langmuir etal 06 GCA
      Al+3 + H3AsO4 = AlH2AsO4+2 + H+
      log_k 0.83

#AlHAsO4+   from Langmuir etal 06 GCA
      Al+3 + H3AsO4 = AlHAsO4+ + 2H+
      log_k -1.91

#AlAsO4   from Langmuir etal 06 GCA
      Al+3 + H3AsO4 = AlAsO4 + 3H+
      log_k -6.6

SURFACE_MASTER_SPECIES
        Goe_uni    Goe_uniOH-0.5
        Goe_tri    Goe_triO-0.5

SURFACE_SPECIES
###############
#  Fe3-O sites
#
        Goe_triO-0.5  = Goe_triO-0.5
             -cd_music  0 0 0 0 0
             log_k 0

        Goe_triO-0.5 + H+ = Goe_triOH+0.5
             -cd_music  1 0 0 0 0
             log_k    9.2

        Goe_triO-0.5 + Na+ = Goe_triONa+0.5
```

```
             -cd_music  0 1 0 0 0
             log_k     -0.6

        Goe_triO-0.5 + K+ = Goe_triOK+0.5
             -cd_music  0 1 0 0 0
             log_k     -1.61

        Goe_triO-0.5 + H+ + Cl- = Goe_triOHCl-0.5
             -cd_music  1 -1 0 0 0
             log_k     8.75

        Goe_triO-0.5 + Ca+2 = Goe_triOCa+1.5
             log_k       2.85
             -cd_music  0.0  2.0  0 0 0

###############
#  Fe-O sites
#
        Goe_uniOH-0.5 = Goe_uniO-0.5
             -cd_music  0 0 0 0 0
             log_k 0

        Goe_uniOH-0.5 + H+ = Goe_uniOH2+0.5
             -cd_music  1 0 0 0 0
             log_k      9.2

        Goe_uniOH-0.5 + Na+ = Goe_uniOHNa+0.5
             -cd_music  0 1 0 0 0
             log_k     -0.6

        Goe_uniOH-0.5 + K+ = Goe_uniOHK+0.5
             -cd_music  0 1 0 0 0
             log_k     -1.61

        Goe_uniOH-0.5 + H+ + Cl- = Goe_uniOH2Cl-0.5
            -cd_music  1 -1 0 0 0
            log_k       8.75

        Goe_uniOH-0.5 + Ca+2 = Goe_uniOHCa+1.5
             log_k       2.85
             -cd_music  0.0  2.0  0 0 0

###############
#   Anions

#   Arsenate

        Goe_uniOH-0.5 + 2H+ + AsO4-3 = Goe_uniOAsO2OH-1.5 + H2O
            log_k      26.62
              -cd_music  0.30 -1.30 0 0 0

        2Goe_uniOH-0.5 + 2H+ + AsO4-3 = (Goe_uniO)2AsO2-2 + 2H2O
            log_k      29.29
              -cd_music  0.47  -1.47  0 0 0

        2Goe_uniOH-0.5 + 3H+ + AsO4-3 = (Goe_uniO)2AsOOH- + 2H2O
             log_k      32.69
             -cd_music  0.58 -0.58 0 0 0

#   Arsenite

        Goe_uniOH-0.5 + H3AsO3 = Goe_uniOAs(OH)2-0.5 + H2O
              log_k      4.91
             -cd_music  0.16  -0.16 0 0 0

        2Goe_uniOH-0.5 + H3AsO3 = (Goe_uniO)2AsOH-1 + 2H2O
              log_k      7.26
             -cd_music  0.34 -0.34 0 0 0

#   Phosphate

        Goe_uniOH-0.5 + 2H+ + PO4-3 = Goe_uniOPO2OH-1.5 + H2O
             log_k       27.65
             -cd_music  0.28 -1.28 0 0 0

        2Goe_uniOH-0.5 + 2H+ + PO4-3 = (Goe_uniO)2PO2-2 + 2H2O
             log_k       29.77
             -cd_music  0.46  -1.46  0 0 0

#   Carbonate

        2Goe_uniOH-0.5 + 2H+ + CO3-2 = (Goe_uniO)2CO- + 2H2O
             log_k      22.33
             -cd_music  0.68  -0.68  0 0 0
```

```
#   Silica

        2Goe_uniOH-0.5 + H4SiO4 = (Goe_uniO)2Si(OH)2-1 + 2H2O
             log_k      5.85
             -cd_music  0.29  -0.29  0 0 0

        2Goe_uniOH-0.5 + 4H4SiO4 = (Goe_uniO)2SiOHOSi3O2(OH)7-1 + 5H2O
             log_k      13.98
             -cd_music  0.29  -0.29  0 0 0

        2Goe_uniOH-0.5 + 4H4SiO4 = (Goe_uniO)2SiOHOSi3O3(OH)6-2 + 5H2O + H+
             log_k      7.47
             -cd_music  0.29  -1.29  0 0 0

###############
#   Cations
#

#   Ferrous iron
        2Goe_uniOH-0.5 + Fe+2 = (Goe_uniOH)2Fe+1
             log_k      8.47
             -cd_music  0.73  1.27  0 0 0

#   Ferrous with surface oxidation to ferric
        2Goe_uniOH-0.5 + Fe+2 + 2H2O = (Goe_uniOH)2Fe(OH)2-1 + 2H+
             log_k      -9.31
             -cd_music  0.17  -0.17  0 0 0

#   Ferrous-arsenite surface complex
        Goe_uniOH-0.5 + Fe+2 + H3AsO3 = Goe_uniOAs(OH)3Fe+0.5 + H+
             log_k      3.38
             -cd_music  0.08  0.92  0 0 0

#   Calcium #inner sphere complexes; outer sphere complexes are defined above

        Goe_uniOH-0.5 + Ca+2 = Goe_uniOHCa+1.5
             log_k      3.69
             -cd_music  0.32  1.68  0 0 0

        Goe_uniOH-0.5 + Ca+2 + H2O = Goe_uniOHCaOH+0.5 + H+
             log_k      -9.17
             -cd_music  0.32  0.68  0 0 0

#   Magnesium

        2Goe_uniOH-0.5 + Mg+2 = (Goe_uniOH)2Mg+1
             log_k      4.89
             -cd_music  0.71  1.29  0 0 0

        2Goe_uniOH-0.5 + Mg+2 + H2O = (Goe_uniOH)2MgOH + H+
             log_k      -6.44
             -cd_music  0.71  0.29  0 0 0
```

PHREEQC FILES USED FOR CH_4 MODELS

PHREEQC INPUT FOR STEPWISE FORWARD MODELLING OF FOCUS AREA

```
DATABASE C:\Program Files (x86)\USGS\Phreeqc Interactive 3.5.0-14000\database\wateq4f.dat
SELECTED_OUTPUT
-file 04_FwMX_CH4_co_d113-700_noN(5)S(6)O(0)_chal.xls # file name
-distance false
-time false
-step false
-solution false
-temperature true
-Alkalinity
-totals O(0) Mg Mn(4) Mn(2) Fe(3) Fe(2) Ca C(4) C(-4) N(5) S(6) As Ba Cu Ni Si Sr Zn
-equilibrium_phases Calcite Siderite Fe(OH)3(a) Ni-Birnessite2 Rhodochrosite Quartz
-saturation_indices Calcite Siderite Rhodochrosite Fe(OH)3(a) Ni-Birnessite2 CO2(g) CH4(g) Quartz

PHASES
Ni-Birnessite1
        Mn0.995Ni0.005O1.995 + 3.99H+ + 1.99e- = 0.995Mn+2 + 0.005Ni+2 + 1.995H2O
        log_k           43.601
Ni-Birnessite2
        Mn0.99Ni0.01O1.99 + 3.98H+ + 1.98e- = 0.99Mn+2 + 0.01Ni+2 + 1.99H2O
        log_k           43.601

SURFACE_SPECIES
#   Nickel
        Hfo_sOH + Ni+2 = Hfo_sONi+ + H+
```

```
        log_k  0.37

        Hfo_wOH + Ni+2 = Hfo_wONi+ + H+
        log_k  -2.5                     # table 10.5
#   Zinc
        Hfo_sOH + Zn+2 = Hfo_sOZn+ + H+
        log_k  0.0 #decreased from 0.99

        Hfo_wOH + Zn+2 = Hfo_wOZn+ + H+
        log_k   -3.0 #decreased from -1.99
#   Copper
        Hfo_sOH + Cu+2 = Hfo_sOCu+ + H+
        log_k 2.89  #inc from 0.78=linear average Ni and Zn - org 2.89

        Hfo_wOH + Cu+2 = Hfo_wOCu+ + H+
        log_k  0.6  #-2.17=linear average Ni and Zn  - org 0.6

SOLUTION_SPREAD #reduced by removing oxidants (SO4 and NO3)
# NOTE for running the file each analyses should be on one line!!
-units mg/l
```

Number	Description	pH	Temp	Alkalinity	C(-4)	Cl	Al	As	Ba	Ca	Cu	Fe	K	Mg	Mn	Na	Ni	Si	Sr	Zn
														mg/l	mg/l	mg/l	mg/l	mg/l	mg/l	mg/l
1	M6-d113	7.16	14.63	230	8.564	0.924	0.053	0.00008	0.017	103.0	0.0040	2.698	0.446	5.532	0.183	5.665	0.000	4.831	0.247	0.0126
2	M6-d127	7.05	11.55	230	12.968		0.681	0.007	0.00006	0.016	99.8	0.0020	1.953	0.428	5.713	0.188	4.624	0.014	4.552	0.226	0.0005
3	M6-d245	7.33	5.68	260	12.894		1.431	0.128	0.00071	0.029	94.7	0.0075	3.074	0.213	3.776	0.145	3.011	0.029	4.962	0.176	0.0229
4	M6-d323	7.18	6.935	266.3	10.874		1.674	0.040	0.00096	0.024	114.6	0.0060	3.376	0.553	5.531	0.139	1.399	0.050	3.547	0.195	0.0136
5	M6-d496	7.17	8.19	272.5	5.000	0.688	0.015	0.00027	0.022	140.4	0.0014	3.353	0.604	10.164		0.288	2.948	0.001	5.864	0.273	0.0002
6	M7-d113	7.18	14.51	230	27.666		2.350	0.092	0.00024	0.020	106.5	0.0029	2.541	0.751	5.638	0.227	11.811		0.001	5.058	0.277	0.0130
7	M7-d127	7.11	11.72	230	15.516		2.546	0.009	0.00012	0.023	101.8	0.0029	2.630	0.724	5.558	0.241	9.240	0.018	4.955	0.279	0.0700
8	M7-d245	7.34	5.77	275	11.770		1.354	0.110	0.00066	0.024	97.1	0.0052	2.793	0.864	3.867	0.160	5.034	0.036	5.063	0.220	0.0034
9	M7-d323	7.27	6.935	280	6.744	2.205	0.043	0.00086	0.019	94.4	0.0056	2.422	1.103	3.613	0.124	0.829	0.046	3.598	0.170	0.0121
10	M8-d113	7.11	14.93	230	20.739		3.991	0.056	0.00011	0.022	122.6	0.0025	3.848	0.711	6.885	0.282	15.476		0.001	5.288	0.357	0.0083
11	M8-d127	7.09	11.59	230	20.962		2.270	0.011	0.00005	0.022	128.2	0.0030	2.674	0.714	6.380	0.280	9.771	0.016	5.197	0.357	0.0014
12	M8-d245	7.33	5.77	267	10.061		2.445	0.025	0.00084	0.023	110.9	0.0048	2.973	0.426	3.776	0.175	6.229	0.030	5.513	0.209	0.0064
13	M8-d496	7.15	7.17	322.5	10.010		0.851	0.011	0.00051	0.023	152.0	0.0022	3.524	1.217	7.554	0.305	2.687	0.002	6.520	0.269	0.0008
14	M8-d700	7.13	13.4	287.5	2.858	3.033	0.012	0.00047	0.013	142.3	0.0009	1.849	0.501	5.919	0.139	2.358	0.000	11.936		0.156	0.0083
15	M11-d113	7.14	14.62	230	2.397	0.796	0.010	0.00008	0.015	108.1	0.0008	2.775	0.454	5.701	0.210	4.979	0.002	5.195	0.232	0.0003
16	M11-d245	7.29	6.41	265	9.319	1.076	0.009	0.00057	0.017	89.7	0.0045	3.710	0.298	3.881	0.202	2.710	0.033	4.908	0.194	0.0015
17	M11-d323	7.31	6.935	295.0	5.000	1.237	0.099	0.00092	0.016	103.8	0.0082	3.141	0.503	4.695	0.147	0.442	0.047	3.599	0.185	0.0215
18	M11-d496	7.13	7.68	325	1.958	0.622	0.012	0.00028	0.022	144.8	0.0024	3.733	0.698	9.842	0.329	3.092	0.001	6.615	0.293	0.0027
19	M11-d700	7.21	12.97	292.5	4.002	0.739	0.010	0.00025	0.010	135.6	0.0009	1.824	0.620	7.666	0.117	2.359	0.000	16.225		0.131	0.0009
20	M12-d113	7.16	14.37	230	12.372		1.233	0.052	0.00019	0.018	107.4	0.0028	3.049	0.579	4.345	0.181	5.225	0.001	5.412	0.213	0.0088
21	M12-d127	7.13	11.93	230	22.436		0.964	0.009	0.00008	0.016	111.5	0.0009	2.130	0.608	4.494	0.196	4.048	0.001	5.376	0.225	0.0002
22	M12-d245	7.34	5.89	245	12.990		1.511	0.010	0.00060	0.020	84.3	0.0044	2.468	0.334	3.387	0.177	2.568	0.031	4.882	0.186	0.0039
23	M12-d323	7.27	6.930	270.0	15.820		2.570	0.059	0.00079	0.020	109.8	0.0071	2.578	1.341	4.311	0.134	1.087	0.045	3.974	0.182	0.0160
24	M12-d496	7.18	7.97	295	11.570		0.865	0.013	0.00038	0.022	135.7	0.0017	2.785	0.802	8.630	0.256	3.050	0.001	6.330	0.259	0.0006
25	M12-d700	7.07	14.83	260	5.225	1.125	0.015	0.00052	0.012	124.3	0.0003	1.627	0.569	6.283	0.100	2.437	0.000	14.187		0.136	0.0132
26	M13-d113	7.11	14.57	230	20.791		0.857	0.064	0.00141	0.024	106.7	0.0020	5.343	1.074	5.060	0.551	5.340	0.002	6.887	0.277	0.0107
27	M13-d127	7.02	11.22	230	22.479		0.716	0.010	0.00063	0.022	107.5	0.0010	5.087	1.094	5.014	0.474	5.023	0.000	6.022	0.297	0.0009
28	M13-d245	7.2	7.04	267	13.978		1.420	0.105	0.00080	0.027	103.9	0.0049	5.320	0.798	3.677	0.314	3.184	0.031	5.509	0.214	0.0094
29	M13-d323	7.23	7.280	293.5	9.319	1.863	0.083	0.00082	0.025	107.7	0.0072	5.189	1.580	4.263	0.263	1.346	0.046	3.858	0.188	0.0235
30	M13-d496	7.14	7.52	320	5.625	0.970	0.012	0.00074	0.035	142.2	0.0018	6.463	2.196	7.868	0.547	3.067	0.002	6.908	0.271	0.0017

```
31    M13-d700    7.2   13.08 245   1.783 1.775 0.010 0.00066     0.019 125.2 0.0001      3.016 0.891
      6.436 0.214 2.511 0.000 14.115      0.157 0.0123
32    M15-d113    7.21  14.57 230   3.508 1.663 0.097 0.00026     0.015 103.6 0.0022      3.365 0.421
      7.971 0.325 11.877      0.001 5.235 0.300 0.0100
33    M15-d127    7.15  11.13 230   3.937 3.355 0.011 0.00015     0.022 103.6 0.0020      3.380 0.420
      8.224 0.345 13.187      0.001 5.304 0.318 0.0010
34    M15-d245    7.43  6.06  267   5.583 1.705 0.015 0.00077     0.027 108.8 0.0054      4.468 0.363
      5.842 0.217 7.011 0.038 5.429 0.234 0.0021
35    M15-d323    7.23  7.185 289.8 2.500 0.733 0.068 0.00067     0.016 111.5 0.0068      3.259 0.372
      5.216 0.192 0.834 0.051 3.875 0.176 0.0184
36    M15-d496    7.18  8.31  312.5 0.322 0.830 0.018 0.00043     0.019 127.6 0.0017      3.426 0.553
      9.934 0.395 3.334 0.001 6.236 0.252 0.0013
37    M15-d700    7.19  13.73 272.5 0.995 0.751 0.011 0.00070     0.009 133.7 0.0004      1.990 0.523
      7.882 0.151 2.363 0.000 15.719      0.126 0.0026
38    M16-d113    7.2   13.95 230   16.269      1.641 0.047 0.00025     0.018 108.1 0.0011      3.010
      0.570 6.545 0.233 9.264 0.001 5.428 0.324 0.0090
39    M16-d127    7.13  8.79  230   21.949      1.324 0.009 0.00004     0.015 105.8 0.0010      2.819
      0.605 5.083 0.193 4.417 0.001 5.407 0.262 0.0005
40    M16-d245    7.36  6     267   14.221      1.873 0.008 0.00065     0.023 105.9 0.0048      3.084
      0.361 3.735 0.144 2.571 0.036 5.758 0.208 0.0017
41    M16-d323    7.22  6.550 281.0 7.000 1.146 0.055 0.00063     0.016 108.1 0.0071      2.870 0.489
      4.261 0.125 0.725 0.053 3.753 0.187 0.0082
42    M16-d496    7.14  7.1   295   9.214 0.731 0.008 0.00026     0.018 108.0 0.0016      2.578 0.466
      6.044 0.189 2.054 0.001 5.037 0.218 0.0012
43    M16-d700    7.2   14.28 245   4.189 1.154 0.017 0.00026     0.012 135.9 0.0016      1.733 0.627
      6.985 0.106 2.639 0.000 15.347      0.150 0.0005

#The samples within the focus area are mixed
MIX 1 #day 113
1     0.125
6     0.125
10    0.125
15    0.125
20    0.125
26    0.125
32    0.125
38    0.125
SAVE solution 101
END

MIX 2 #day 127
2     0.142847143
7     0.142847143
11    0.142847143
21    0.142847143
27    0.142847143
33    0.142847143
39    0.142847143
SAVE solution 102
END

MIX 3 #day 245
3     0.125
8     0.125
12    0.125
16    0.125
22    0.125
28    0.125
34    0.125
40    0.125
SAVE solution 103
END

MIX 4 #day 323
4     0.142847143
9     0.142847143
17    0.142847143
23    0.142847143
29    0.142847143
35    0.142847143
41    0.142847143
SAVE solution 104
END

MIX 5 #day 496
5     0.142847143
13    0.142847143
18    0.142847143
24    0.142847143
30    0.142847143
36    0.142847143
42    0.142847143
SAVE solution 105
END
```

```
MIX 6 #day 700
14    0.166666667
19    0.166666667
25    0.166666667
31    0.166666667
37    0.166666667
43    0.166666667
SAVE solution 106
END

#-------------------------------------------------------------------------------------------
#values to add because they were removed prior to mix
#mol O(0)         Day  solution
#1.10641E-05      113   101
#1.30559E-05      127   102
#0.000108834      245   103
#1.04358E-05      323   104
#0.000258079      496   105
#0.00013109       700   106

#Forward modelling sulfate and nitrate have been removed
#Day 113-127
USE solution 101

SURFACE 101
Hfo_w  0.04  600  10 #Dw 1e-13
Hfo_s  1e-4
-equilibrate  101

EQUILIBRIUM_PHASES 101
Calcite -0.0891
Quartz 0.17

REACTION 101
CH4 0.00044
O2 0.000651 #0.000011 previously removed has been readded

REACTION_TEMPERATURE 101
11.133

END
#_____________________________________________________________________
#Forward modelling
#Day 127-245
USE solution 102

#SURFACE 102
#Hfo_w  0.04  600  10 #Dw 1e-13
#Hfo_s  1e-4
#-equilibrate  102

SURFACE 102
Hfo_w  Fe(OH)3(a) equilibrium_phase 0.2  5.33e4 #Dw 1e-13
Hfo_s  Fe(OH)3(a) equilibrium_phase 5e-3
-equilibrate  102 # equilibrate with solution 1

EQUILIBRIUM_PHASES 102
Calcite 0.0858
Fe(OH)3(a) -4 0.0020 #increased from 0.00125 to compensate for extra metanox
             #0.0004 is average of oxalate extract core S1 Ni/Fe in oxalate (S1) 0.00038
Siderite 0.7216 0.0005
Rhodochrosite -0.2062 0
Quartz 0.17

REACTION 102
CH4 0.00142  #changed from 0.00062 to get more Alkalinity
O2 0.002913 #changed from 0.001513 to get more Alkalinity
             #0.000013 previously removed has been readded
Ni-Birnessite1 0.00009

REACTION_TEMPERATURE 102
6.078

END
#-------------------------------------------------------------------
#Forward modelling
#Day 245-323
USE solution 103

SURFACE 103
Hfo_w  0.04  600  10 #Dw 1e-13
Hfo_s  1e-4
-equilibrate  103

EQUILIBRIUM_PHASES 103
```

```
Calcite 0.0734
Quartz 0.17

REACTION 103
CH4 0.002
O2 0.00439 #0.00109 previously removed has been readded

REACTION_TEMPERATURE 1
6.964

END

#-----------------------------------------------------------------------
#Forward modelling
#Day 323-496
USE solution 104

SURFACE 104
Hfo_w  Fe(OH)3(a) equilibrium_phase 0.2  5.33e4 #Dw 1e-13
Hfo_s  Fe(OH)3(a) equilibrium_phase 5e-3
-equilibrate  104 # equilibrate with solution 104

EQUILIBRIUM_PHASES 104
Calcite 0.1136
Fe(OH)3(a) 0 0.00005 precipitation only # tiny bit left - new forms by Fe oxidation (of the siderite)
Siderite 0.55 0.00010 dissolution only
Rhodochrosite 0.0 0.00007 dissolution only
Ni-Birnessite2 0 0.0001 precipitation only #to avoid reduction
Quartz 0.17

REACTION 104
CH4 0.00005  #increased from 0
O2 0.0011904 #0.0000104 previously removed has been readded

REACTION_TEMPERATURE 1
7.706

SAVE solution 111
SAVE surface 111
END

#-----------------------------------------------------------------------
#Forward modelling
#Day 496-700
USE solution 105

SURFACE 105
Hfo_w  0.04  600  10 #Dw 1e-13
Hfo_s  1e-4
-equilibrate  105

EQUILIBRIUM_PHASES 105
Calcite 0.1554
Quartz 0.17

REACTION 105
CH4 0.000016
O2 0.000258 #0.000258 previously removed has been readded

REACTION_TEMPERATURE 1
13.715
END
A
```

PHREEQC MODEL FOR MODELLING THE ATTENUATION OF METHANE IN THE AQUIFER FOR THE INJECTION EXPERIMENT

```
DATABASE C:\Program Files (x86)\USGS\Phreeqc Interactive 3.5.0-14000\database\wateq4f.dat
PRINT
  -reset false
  -echo_input true
  -status true
SELECTED_OUTPUT
-file CH4Extent3,9mMCH4(g)_03UnlimO2_Lin(0).xls # file name
-temperature true
-Alkalinity
-totals O(0) Mg Mn(4) Mn(2) Fe(3) Fe(2) Ca C(4) C(-4) N(5) S(6) As Ba Cu Ni Si Sr Zn
-equilibrium_phases Calcite Siderite Fe(OH)3(a) Ni-Birnessite2 Rhodochrosite CH4(g) Quartz
-saturation_indices Calcite Siderite Rhodochrosite Fe(OH)3(a) Ni-Birnessite2 CO2(g) CH4(g) Quartz
-kinetic_reactants OxygenAdd

#Transport model - 0.25 cm cell 5 cm/d i.e 5 days/shift
```

```
RATES #Very simply rate expression calculating rate of O2 addition that reacts immediately based on
the amount of CH4 available - since there seems to be a dependency
# when O2 reaches 50% of saturation the rate goes to zero so no more Oxygen is added
OxygenAdd
-start
8 IF MOL("O2") > 0.000156 THEN GOTO 78
10 rate = 0.0185 * MOL("CH4")/86400 #moles/l/day converted to /second #slope from y(0)=0
70 moles = rate * TIME
71 GOTO 80
78 moles = 0
79 GOTO 90
80 IF moles > SYS("C(-4)") THEN moles = M
90 SAVE moles
-end

SOLUTION 0 Background solution from before injection - day 2 with adjustments for missing parameters
     -units mg/l
      pH    7.23
      -temp 16.19
      Alkalinity  204
      As    0.061
      Ca    91.86168388 #from day -49
      Fe(2) 3 #from day -49
      Mg    3.52735
      Mn    0.422053
      Na    4.09044
      Ni    0.135069667
      Si    1.56303
      Zn    1.27074
      Br    0.0079904

SOLUTION 1-24  M7-d113 cells 1-24 represent a patch of high concentration (-3-+3 m in the test field)
with a similar amount of CH4 present as an equilibrium phase
pH    7.18
Temp  14.51
Alkalinity  230
C(-4) 27.666 CH4(g) 0.02 #the SI of 0.2 gives a concentration close to the measured a good indication
of methane bubbles in equilibrium with the water at shallow depth (0.2 corresponds to 1.047 atm
Cl    2.35
Al    0.092
As    0.00024
Ba    0.02
Ca    106.5
Cu    0.0029
Fe    2.541
K     0.751
Mg    5.638
Mn    0.227
Na    11.811
Ni    0.001
Si    5.058
Sr    0.277
Zn    0.013

EQUILIBRIUM_PHASES 1-24 #the "bubble of methane in the first -3 to +3 meters
CH4(g) 0.02 0.00386  # - 0.00386 mmol/l is the output of the forward model - SI 0.02 (log(P(CH4)=0.2)
also corresponds to measured concentration

SOLUTION 25-60 Background solution 3-12 m from injection - from before injection - day 2 with
adjustments for missing parameters
      -units mg/l
      pH    7.23
      -temp 16.19
      Alkalinity  204
      As    0.061
      Ca    91.86168388 #from day -49
      Fe(2) 3 #from day -49
      Mg    3.52735
      Mn    0.422053
      Na    4.09044
      Ni    0.135069667
      Si    1.56303
      Zn    1.27074


KINETICS 1-60 # Influx of oxygen in the whole system
OxygenAdd
-formula O2  1
-M0  10
-cvode true

TRANSPORT
        -cells               60 #15 meters -3 - +12 meters
        #-stagnant          1 6.8e-6 0.3 0.05
        -lengths             0.25
```

```
        -shifts               320  #1600 days
        -time_step            432000 #5 days flowrate 5 cm/day
        -flow_direction       forward
        -boundary_conditions  flux flux
        -dispersivities       0.01
        -correct_disp         true
        -diffusion_coefficient 5e-10
        -punch_frequency      3 #every 15 days
END
```

PHREEQC MODEL FOR MODELLING THE ATTENUATION OF METHANE IN THE AQUIFER AFTER A 100 DAY LEAK AT 4 M3/D

```
DATABASE C:\Program Files (x86)\USGS\Phreeqc Interactive 3.5.0-14000\database\wateq4f.dat
PRINT
    -reset false
    -echo_input true
    -status true
SELECTED_OUTPUT
-file CH4Extent3,9mMCH4(g)_03_500m_unlimO2_Lin(0).xls # file name
#-distance false
#-time false
#-step false
#-solution false
-temperature true
-Alkalinity
-totals O(0) Mg Mn(4) Mn(2) Fe(3) Fe(2) Ca C(4) C(-4) N(5) S(6) As Ba Cu Ni Si Sr Zn
-equilibrium_phases Calcite Siderite Fe(OH)3(a) Ni-Birnessite2 Rhodochrosite CH4(g) Quartz
-saturation_indices Calcite Siderite Rhodochrosite Fe(OH)3(a) Ni-Birnessite2 CO2(g) CH4(g) Quartz
-kinetic_reactants OxygenAdd

#Large Leak Transport model - 100 cm cells 5 cm/d i.e 20 days/shift 500 m

RATES #Very simply rate expression calculating rate of O2 addition that reacts immediately based on
#the amount of CH4 available - since there seems to be a dependency
# when O2 reaches 0.000156 (50% of saturation at 10 degrees)
#the rate goes to zero so no more Oxygen is added

OxygenAdd
-start
8 IF MOL("O2") > 0.000156 THEN GOTO 78
10 rate = 0.0185 * MOL("CH4")/86400 #moles/l/day converted to /second
70 moles = rate * TIME
71 GOTO 80 # skips nex line unless coming directly from line 8
78 moles = 0
79 GOTO 90
80 IF moles > SYS("C(-4)") THEN moles = M
90 SAVE moles
-end


SOLUTION 0 Background solution from before injection - day 2 with adjustments for missing parameters
      -units mg/l
      pH    7.23
      -temp 16.19
      Alkalinity  204
      As    0.061
      Ca    91.86168388 #from day -49
      Fe(2) 3 #from day -49
      Mg    3.52735
      Mn    0.422053
      Na    4.09044
      Ni    0.135069667
      Si    1.56303
      Zn    1.27074
      Br    0.0079904

SOLUTION 1-300  M7-d113 cells 1-300 represent a patch of high concentration with a similar amount of
CH4 present as an equilibrium phase
pH    7.18
Temp  14.51
Alkalinity  230
      C(-4) 27.666 CH4(g) 0.02 #the SI of 0.2 gives a concentration close to the measured
            # a good indication of methane bubbles in equilibrium with the water at
            # shallow depth (0.2 corresponds to 1.047 atm)
Cl    2.35
Al    0.092
As    0.00024
Ba    0.02
Ca    106.5
Cu    0.0029
Fe    2.541
K     0.751
Mg    5.638
Mn    0.227
```

```
Na    11.811
Ni    0.001
Si    5.058
Sr    0.277
Zn    0.013

EQUILIBRIUM_PHASES 1-300 #the "bubble" of methane caused by 100 day leak  at 4.3 m3/day
                  #- extrapolated from the 6 m "bubble" caused by the 2 day leak in the experiment
CH4(g) 0.02 0.0039  # - 0.00386 is the gas phase methane derived from the forward model
                #- SI 0.02 also corresponds to measured concentration

SOLUTION 301-500 Background solution 3-12 m from injection - from before injection - day 2 with
adjustments for missing parameters
      -units mg/l
      pH    7.23
      -temp 16.19
      Alkalinity  204
      As    0.061
      Ca    91.86168388 #from day -49
      Fe(2) 3 #from day -49
      Mg    3.52735
      Mn    0.422053
      Na    4.09044
      Ni    0.135069667
      Si    1.56303
      Zn    1.27074

KINETICS 1-500 # Influx of oxygen in the whole system - amount set to unlimited
               # (10 moles) because when CH4 is gone the rate goes to 0
OxygenAdd
-formula O2  1
-M0  10
-cvode true


TRANSPORT
        -cells                 500 #length 1 m = 500 meters
        #-stagnant            1 6.8e-6 0.3 0.05
        -lengths               1
        -shifts                100  #2000 days
        -time_step             1728000 #20 days flowrate 5 cm/day
        -flow_direction        forward
        -boundary_conditions   flux flux
        -dispersivities        1
        -correct_disp          true
        -diffusion_coefficient 5e-10
        -punch_frequency       1 #every 20 days - next line means only every 10 m i punched
        -punch    0 10 20 30 40 50 60 70  80 90 100 110 120 130 140 150 160 170 180 190  200 210 /
                220 230 240 250 260 270 280 290 300 310 320 330 340 350 360 370 380 390 400 410 /
             420 430 440 450 460 470 480 490 500 #510 520 530 540 550 560 570 580 590 600 610 620 /
             630 640 650 660 670 680 690 700 710 720 730 740 750 760 770 780 790 800
END
```

6 References

BENSON, S. AND HEPPLE, R. (2005) 'Prospects for Early Detection and Options for Remediation of Leakage from CO2 Storage Projects', *Carbon Dioxide Capture for Storage in Deep Geologic Formations*, 2, pp. 1189–1203. doi: 10.1016/B978-008044570-0/50157-4.

CAHILL, A. G., STEELMAN, C. M., FORDE, O., KULOYO, O., EMIL RUFF, S., MAYER, B., ULRICH MAYER, K., STROUS, M., CATHRYN RYAN, M., CHERRY, J. A. AND PARKER, B. L. (2017) 'Mobility and persistence of methane in groundwater in a controlled-release field experiment', *Nature Geoscience*, 10(4), pp. 289–294. doi: 10.1038/ngeo2919.

CAHILL, A.G. AND JAKOBSEN, R. (2015) 'Geochemical modeling of a sustained shallow aquifer CO2 leakage field study and implications for leakage and site monitoring', *International Journal of Greenhouse Gas Control*, 37. doi: 10.1016/j.ijggc.2015.03.011.

CAHILL, AARON G. AND JAKOBSEN, R. (2015) 'Geochemical modeling of a sustained shallow aquifer CO2 leakage field study and implications for leakage and site monitoring', *International Journal of Greenhouse Gas Control*, 37, pp. 127–141. doi: 10.1016/j.ijggc.2015.03.011.

CAHILL, A. G., MARKER, P. AND JAKOBSEN, R. (2014) 'Hydrogeochemical and mineralogical effects of sustained CO2 contamination in a shallow sandy aquifer: A field-scale controlled release experiment', *Water Resources Research*, 50(2). doi: 10.1002/2013WR014294.

FORDE, O. N., CAHILL, A. G., MAYER, K. U., MAYER, B., SIMISTER, R. L., FINKE, N., CROWE, S. A., CHERRY, J. A. AND PARKER, B. L. (2019) 'Hydro-biogeochemical impacts of fugitive methane on a shallow unconfined aquifer', *Science of the Total Environment*, 690(2019), pp. 1342–1354. doi: 10.1016/j.scitotenv.2019.06.322.

VAN GENUCHTEN, C. M., BEHRENDS, T., STIPP, S. L. S. AND DIDERIKSEN, K. (2020) 'Achieving arsenic concentrations of <1 µg/L by Fe(0) electrolysis: The exceptional performance of magnetite', *Water Research*, 168. doi: 10.1016/j.watres.2019.115170.

HIEMSTRA, T. AND VAN RIEMSDIJK, W. H. (2006) 'On the relationship between charge distribution, surface hydration, and the structure of the interface of metal hydroxides', *Journal of Colloid and Interface Science*, 301(1), pp. 1–18. doi: 10.1016/j.jcis.2006.05.008.

JESSEN, S., POSTMA, D., LARSEN, F., NHAN, P. Q., HOA, L. Q., TRANG, P. T. K., LONG, T. V., VIET, P. H. AND JAKOBSEN, R. (2012) 'Surface complexation modeling of groundwater arsenic mobility: Results of a forced gradient experiment in a Red River flood plain aquifer, Vietnam', *Geochimica et Cosmochimica Acta*, 98. doi: 10.1016/j.gca.2012.07.014.

LARSEN, F. AND POSTMA, D. (1997) 'Nickel mobilization in a groundwater well field: Release by pyrite oxidation and desorption from manganese oxides', *Environmental Science and Technology*, 31(9), pp. 2589–2595. doi: 10.1021/es9610794.

PALANDRI, J. L. AND KHARAKA, Y. K. (2004) 'A compilation of rate parameters of water-mineral interaction kinetics for application to geochemical modeling', *USGS Open File Report*, 2004–1068, p. 71. Available at: http://www.dtic.mil/cgi-bin/GetTRDoc?Location=U2&doc=GetTRDoc.pdf&AD=ADA440035.

PARKHURST, D. L. AND APPELO, C. A. J. (2013) 'PHREEQC (Version 3.0. 4)--A computer program for speciation, batch speciation, one-dimensional transport, and inverse geochemical calculations', *US Geological Survey Techniques and Methods, Book*, 6, p. 497.

POSTMA, D., PHAM, T. K. T., SØ, H. U., HOANG, V. H., VI, M. L., NGUYEN, T. T., LARSEN, F., PHAM, H. V. AND JAKOBSEN, R. (2016) 'A model for the evolution in water chemistry of an arsenic contaminated aquifer over the last 6000 years, Red River floodplain, Vietnam', *Geochimica et Cosmochimica Acta*, 195. doi: 10.1016/j.gca.2016.09.014.

YANG, S., LV, Y., LIU, X., WANG, Y., FAN, Q., YANG, Z., BOON, N., WANG, F., XIAO, X. AND ZHANG, Y. (2020) 'Genomic and enzymatic evidence of acetogenesis by anaerobic methanotrophic archaea', *Nature Communications*, 11(1), pp. 1–11. doi: 10.1038/s41467-020-17860-8.

ZHANG, Y., HU, B., TENG, Y., TU, K. AND ZHU, C. (2019) 'A library of BASIC scripts of reaction rates for geochemical modeling using PHREEQC', *Computers and Geosciences*, 133(December 2018), p. 104316. doi: 10.1016/j.cageo.2019.104316.